Impacts of SDF-1 and Radiation Dose-Rate in an Adult Zebrafish Model of Hematopoietic Cell Transplant

A DISSERTATION
SUBMITTED TO THE FACULTY OF
UNIVERSITY OF MINNESOTA
BY

Tiffany Glass

IN PARTIAL FULFILLMENT OF THE REQUIREMENTS
FOR THE DEGREE OF
DOCTOR OF PHILOSOPHY

Bruce Blazar, Adviser

May 2013

Acknowledgements

I would like to thank the individuals and groups that assisted and supported this work.

Bruce Blazar made this research happen through his roles as mentor and advisor. Bruce has shaped my development as a research scientist, and I deeply appreciate the excellent training and research environment that he has provided.

Troy Lund acted as a close technical and scientific advisor and collaborator. He designed the DNA construct that was used to create the Tg(*sdf-1a:DsRed*) zebrafish, and also designed the *sdf-1* in situ probes used in this work.

The bulk of chapter 2 has been previously published with the close assistance of co-authors Troy Lund, Teresa Bowman, Leonard Zon, Xiaobai Patrinostro, Jakub Tolar, and Bruce Blazar: Stromal cell-derived factor-1 and hematopoietic cell homing in an adult zebrafish model of hematopoietic cell transplantation. Blood. 2011 Jul 21;118(3):766-74. © the American Society of Hematology.

Susanta Hui conducted all preconditioning radiation of zebrafish that required a linear accelerator. This represented a substantial investment of time on his part.

This work was assisted in many ways by the University of Minnesota Zebrafish Core. Without this core facility, none of this research would have been possible.

Finally, I would like to thank my committee members; Lisa Schimmenti, Yoji Shimizu, Brian Fife, Bryce Binstadt, and Kristin Hogquist, for their generosity with their time and advice. I particularly appreciated the willingness of Yoji and Chris DeNucci to discuss the technical considerations involved in cell adhesion assays.

Dedication

This dissertation is dedicated to the patients whose travails necessitate biomedical research, and to the model organisms who give their lives for it.

Abstract

Despite a history of refinements, Hematopoietic Cell Transplant (HCT) remains a potentially difficult treatment that can have high risks for complications and mortality. We used adult zebrafish models of HCT to study two broad biological processes that occur during HCT; homing and early donor-derived hematopoietic reconstitution. In the first case, we validated the adult zebrafish model for the study of the chemokine SDF-1 in HCT, developed a transgenic *sdf-1* reporter zebrafish line, and used it to determine sites of high *sdf-1* expression in recipient organisms. These sites were discovered both in the hematopoietic tissue as well as in previously un-described structures throughout the skin, and were found to consistently attract donor-derived cells after transplant. Ultimately, this allowed the identification of new putative HSC-niche cells which can be isolated with relative ease. Secondly, we assessed the effects of high conditioning radiation dose-rates on the process of hematopoietic engraftment after transplant. In groups of adult zebrafish given the same total dose of preconditioning radiation, we found that recipients irradiated at a high rate show significantly faster engraftment compared to those irradiated at a lower rate. Insights offered by this work will contribute to future efforts identifying endogenous factors promoting rapid engraftment, as well as to future reassessments of therapeutic opportunities offered by biologically informed refinements of preconditioning radiation strategies.

Table of Contents

List of Figures

Chapter 1

Chapter 2.

Chapter 3.

Chapter 4.

Chapter 1. Introduction

HSPC Homing

In Hematopoietic Cell Transplant (HCT), patients' immune and hematopoietic cells are suppressed or ablated with preconditioning radiation and chemotherapy, and patients are given infusions of donor hematopoietic stem cells (HSC). Immediate migration of transplanted HSC to the bone marrow is a crucial process for ultimately achieving donor-derived reconstitution of the hematopoietic system. While homing in this context can refer to donor cell migration to the bone marrow over a time range spanning anywhere from a few minutes to two days after transplant, it has been used by some investigators to account for the presence of donor cells in the bone marrow at least as late as five days after transplant [1-3].

Several biological steps in this migration process have been documented in murine models of HCT. After infusion of HSC into the circulation, the cells actively move from the circulation to HSC niche sites in the bone marrow and spleen through the multistep process of rolling along the vessel lumen, adhering to the vessel wall, extravasating through the endothelium, and ultimately migrating through the tissue to a final niche site. The cell-cell interaction steps of this process are mediated by integrin heterodimers and E- and P-selectin interactions between HSC and endothelial cell surfaces, while the process additionally relies on chemokines for integrin activation and directional cell guidance [4 5 6]. HSC mobilization from the stem cell niche into the circulation, and

homing from the circulation to the bone marrow, routinely occur endogenously as a normal aspect of hematopoietic homeostasis [7]. Because of this, it is reasonable to expect that pre-existing endogenous mechanisms help to drive the homing of donor HSC during HCT.

Since homing has been of perceived importance to HCT outcome, there has been interest in identifying the mechanisms that promote it, and avenues for therapeutically enhancing it. Broadly, these efforts seek to improve homing first by synergizing with endogenous cues that attract migrating HSC to sites that promote hematopoietic survival and proliferation, and secondly by clearing recipient hematopoietic cells from the HSC niche sites, thereby making the sites available to retain transplanted cells. The oldest method to accomplish these broad goals, which was by necessity applied in the very first successful bone marrow transplants, is preconditioning radiation [8].

Radiation conditioning can be a powerful method for strategically eliciting biological changes from recipient tissues and is still used today after a long history of refinements. However, the precise effects of radiation on homing can be complex, and are occasionally a topic of some dispute amongst investigators. The biological consequence of radiation treatment that was the first to be recognized as integral to the bone marrow transplant process is the suppression or ablation of recipient hematopoietic cells; native to the patient [8]. Beyond that impact, subsequent studies have reported evidence that radiation treatment causes up-regulation of endogenous mediators of HSPC migration, which may

enhance homing of donor cells following transplant [9] [10]. Other groups, however, have reported that donor HSPC homing to bone marrow after transplant in irradiated mice is actually substantially less than HSPC homing in non-irradiated mice [1,11]. These seeming discrepancies might be resolved by considering that increasing intensity and area of radiation conditioning can enhance homing of donor cells up to a point, beyond which the consequences of mounting toxicities and cell damage may be counterproductive. Examples of off-target radiation responses that may interfere with homing to bone marrow include the radiation-induced upregulation of chemoattractants and endothelial adhesion factors in peripheral, non-hematopoietic tissues, which can promote extramedullary migration of transplanted cells, thereby reducing the number of HSC that ultimately reach the bone marrow. The topic is complicated by the fact that biological responses to conditioning radiation can show unpredictable individual variability patient-to-patient, depending on medical history, pre-existing disease, status of other concurrent treatments, and genetic predispositions that modulate radiation sensitivity [12].

Despite this, continued interrogation of radiation conditioning responses and endogenous mechanisms for chemokine-dependent hematopoietic migration processes remain promising avenues for basic investigation that may ultimately suggest new opportunities for therapeutic improvements.

Early Hematopoietic Reconstitution and Engraftment

After successful homing to HSC niche regions of hematopoietic organs, donor HSC must proliferate in order to reconstitute the hematopoietic system.

Studies of early hematopoietic proliferation in mouse models of HCT have identified a few time points after transplant that are generally regarded to be standard for assessing the hematopoietic proliferation and reconstitution process. Historically, the presence of hematopoietic proliferation was frequently detected by observing hematopoietic colonies in the spleen. Although careful investigation provided evidence of hematopoietic proliferation beginning as early as 2 days after transplant, stem and progenitor cells were discovered to give rise to macroscopic spleen-colony formations that could be easily counted 9 or 12 days after transplant, and assays of these time-point to quantify evidence for proliferation have been widely used [13] [14]. Newer approaches using longitudinal *in-vivo* bioluminescent imaging of hematopoietic reconstitution from HSC have also revealed that readily detectible levels of focal, localized hematopoietic proliferation emerge at 9-10 days after transplant in mice, in sites throughout the bone marrow and spleen[15].

Clinical studies suggest that in humans, the amount of time elapsing between cell infusion and indications of significant hematopoietic proliferation can be similar to the time ranges reported for mice. Autologous hematopoietic transplants, in which rejection processes are not applicable to speed of hematopoietic reconstitution, have shown platelet and granulocyte recovery time

means at 11-12 days after myeloablation and infusion of HSC [16,17]. Additionally, daily sample collections in one study to determine early engraftment kinetics in clinical allogenic transplants indicated evidence for increases in donor-derived cells at comparable times, with donor-derived material dominating recipient-derived material at a median of 8 days after transplant as detected by sensitive PCR-based peripheral blood assays[18]. However, early hematopoietic reconstitution kinetics might reflect not just rates of hematopoiesis, but also the emergence of rejection processes, which are typically led by T-cells [19,20]. Graft rejection can happen quickly, and a molecular study of daily peripheral blood samples reports HCT cases in which rejection began to occur at or shortly after 13 days post transplant, and could unfold from initiation (the first detected shift from primarily donor-derived to recipient-derived cells in circulation) to full resolution (autologous recovery, and donor-derived cells no longer detectible) over the course of just 24 hours [18]. Additionally, a clinical study of engraftment in allogenic HCT following nonmyeloablative conditioning found low donor T-cell chimerism at 14 dpt to be predictive of rejection and graft failure [21]. These time frames are consistent with the amount of time typically reported to elapse between initial antigen exposure and adaptive T-cell-mediated rejections. To summarize, previous studies collectively suggest that in the absence of prior recipient sensitization to donor antigens, dramatic evidence of donor-derived cell proliferation after transplant may generally be anticipated to emerge early in the

second week after transplant, with rejection processes, if applicable, potentially manifesting shortly thereafter.

Because of their importance to HCT outcome, early cell proliferation and reconstitution events have also been the target of translational research efforts, with goals of increasing the speed of hematopoietic reconstitution. Efforts at therapeutic approaches to promoting rapid hematopoietic expansion in vivo after HCT have included treatments with G-CSF and KGF [22-25]. A few factors found to be endogenously up-regulated by radiation pre-conditioning also have known roles in promoting hematopoietic proliferation, including G-CSF, and SDF-1[26,27].

Roles of SDF-1 in Homing and Reconstitution

SDF-1 (CXCL12) is involved in several aspects of HSPC migration and proliferation. SDF is an acronym for 'Stromal Cell Derived Factor', named for the in vitro culture of bone marrow-derived cells that gave rise to its discovery [28]. The hematopoietic function of SDF-1 was initially characterized in terms of its role in B-cell development [29], but it has also been reported to contribute to T-cell and myeloid hematopoiesis, albeit to a lesser extent [30]. Although loss of function of SDF-1 and, separately, CXCR4, both cause embryonic lethal phenotypes in mice, embryos show hematopoietic and vascular deficits [30,31].

SDF-1 is a robust chemoattractant for a wide variety of cells, and forms concentration gradients in vivo that elicit directionality in cell migrations in several contexts [32,33]. SDF-1 is particularly prominent in its role inducing transendothelial

migration, since in addition to attracting cells that express CXCR4, it helps to activate integrins on cell surfaces, thereby promoting vascular egress [6]. SDF-1 is prominently expressed at HSC niche sites, where it assists in attraction and retention of HSC. The importance of this chemokine for HSC homing is broadly confirmed by findings that circadian oscillations of SDF-1 levels in the bone marrow cause alternating cycles of endogenous HSC moblilization and homing [7].

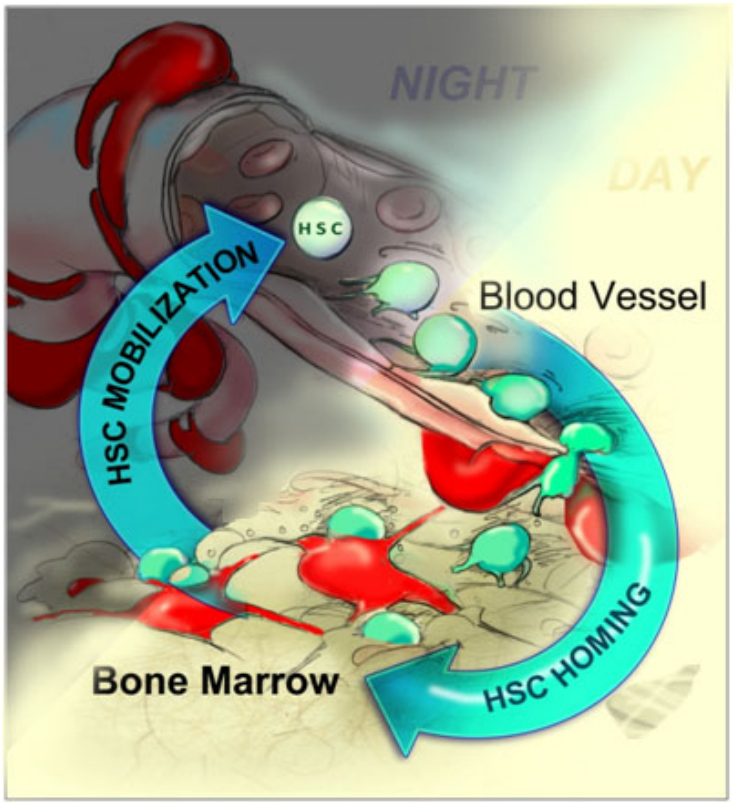

Figure 1. SDF-1 orchestrates mobilization and homing.

Bone marrow cells that express SDF-1 (red) attract and release circulating HSC.

Because of its relevance to the cell migration and proliferation processes necessary for HCT, the SDF-1/CXCR4 axis has been the target of therapeutic modulation. AMD3100, a reversible antagonist of CXCR4, can be used clinically to mobilize HSPC from the bone marrow to the circulation[34]. In mouse models, treatments with AMD3100 after transplant have improved survival and multi-lineage donor-derived cell repopulation. These effects were attributed in part to the drug's capacity to ameliorate cytokine storm and to improve HSC niche availability, thereby promoting donor-derived hematopoietic proliferation and overall improved outcomes [35]. In light of this history, the biology of the SDF-1/CXCR4 axis remains a compelling milieu for efforts to better understand and ultimately improve homing and reconstitution following HCT.

The Zebrafish Models of HSPC Migration and Reconstitution

Despite the obvious differences between fish and mammals, zebrafish show remarkable similarities to mice and humans in aspects of basic biology that are highly pertinent to HCT. These similarities include broadly comparable innate and adaptive immune systems. Although relatively recently established for studies of this nature, zebrafish have become increasingly popular in recent years because they are more logistically amenable to particular routes of discovery that are difficult and expensive to execute using traditional mouse models. Since the size and cost of a zebrafish is a fraction of the cost and size of a mouse, general strategies favoring larger sample sizes and high-throughput or high-risk yet

potentially high-yield experiments can become more financially feasible. Drug screens to identify novel compounds of potential therapeutic benefit, or to reveal novel therapeutic applications for previously studied compounds, are examples of high-throughput experimental paradigms for which the zebrafish are exceptionally well-suited [36,37].

Chemical screens using zebrafish recently highlighted the therapeutic potential of Prostaglandin E2 for promoting HSC proliferation, which has led to clinical trials testing application of this finding to improving engraftment in HCT [38,39]. Zebrafish are also showing excellent potential for use in high-throughput screening of compounds to treat cancer, and to modulate biological responses to radiation [40,41].

Secondly, zebrafish offer more technically straightforward *in-vivo* imaging opportunities than are available in mammalian models. Several previous studies have advanced knowledge of hematopoietic biology through image-based experiments that were relatively easily carried out in zebrafish, but would have been quite technically difficult in mice. These have included *in vivo* tracking of pre-lymphocytes from the primary hematopoietic tissue to the thymus in the developing organism, real-time tracking of migrating HSC within the primary hematopoietic tissue, and *in vivo* observation of cell differentiation events as marked by concurrent expression of fluorophores driven by lineage-specific promoters [42,43].

However, the use of zebrafish for HCT investigation can also present some technical and scientific hurdles to discovery. First, several useful experimental techniques and research reagents that took years to develop and optimize in murine models have yet to attain similar levels of resolution and efficacy for use in the zebrafish model. Within the context of hematopoietic research, examples of useful techniques that are routine in murine investigations yet still technically difficult in zebrafish investigations include ficoll density gradient cell separation techniques (perhaps due to their nucleated erythrocytes, zebrafish blood cells do not separate as neatly in ficoll gradients as do mammalian cells), antibody staining of specific hematopoietic populations (although improving, there are fewer commercially available hematopoietic antibodies available for zebrafish than for mouse), and *in vitro* hematopoietic tools such as lymphocyte proliferation assays. The technical repertoire available for this model is steadily improving, however, as evidenced by frequent reports of technique development to allow approximations of methods used in mammalian inquiries to be applied successfully in zebrafish [44-46]. Secondly, our foundation of basic knowledge of organism-specific anatomy and biology is currently somewhat limited for the zebrafish compared to what is known of the mouse. For example, the anatomy of the embryonic murine lymphatic system has been known since 1975, whereas a zebrafish lymphatic system was not discovered to exist until 2006.[47,48] Thirdly, due to a historical genome duplication event, zebrafish often have at least two similar but not identical genes that correlate to a

sole human orthologue [49]. These orthologues in fish may have divergent expression patterns and function, such that inquiries which would be single-gene efforts in mice or humans will often require interrogation of two or more genes when carried out in the zebrafish.

Despite the added complexity, such genetic redundancy can occasionally offer useful opportunities for interrogation. For example, although loss-of-function mutations in CXCR4 are embryonic lethal in mice, zebrafish that are homozygous for loss of function mutations in one of the two CXCR4 genes are viable yet hematopoietically impaired; thereby providing a unique experimental tool[50]. All of these points collectively create an important consideration for current work in this organism: efforts which require initiating new directions of research in the zebrafish model must often be prefaced by more basic model-specific studies of pertinent biological and logistical considerations.

Chapter 2.

SDF-1 Directs Hematopoietic Cell Migration and Homing in the Adult Zebrafish Model of Hematopoietic Cell Transplant.

Foreword

In mammals, stromal cell-derived factor-1 (SDF-1) promotes hematopoietic cell mobilization and migration. Although the zebrafish, *Danio rerio*, is an emerging model for studying hematopoietic cell transplantation (HCT), the role of SDF-1 in the adult zebrafish has yet to be determined. We sought to characterize *sdf-1* expression and function in the adult zebrafish in the context of HCT. *In-situ* hybridization of adult zebrafish organs shows *sdf-1* expression in kidney tubules, gills, and skin. Radiation upregulates *sdf-1* expression in kidney; to nearly four fold after 40 Gy. Assays indicate that zebrafish hematopoietic cells migrate toward Sdf-1, with a migration ratio (the number of chemoattracted cells divided by the number of passively dispersed cells) approaching 1.5 *in vitro*. A *sdf-1a:DsRed2* transgenic zebrafish allows *in vivo* detection of *sdf-1a* expression in the adult zebrafish. Matings with transgenic reporters localized *sdf-1a* expression to the putative hematopoietic cell niche in proximal and distal renal tubules and collecting ducts. Importantly, transplant of hematopoietic cells into myelosuppressed recipients indicated migration of hematopoietic cells to *sdf-1a* expressing sites in the kidney and skin. We conclude that *sdf-1* expression and function in the adult zebrafish has important similarities to mammals and this *sdf-1* transgenic vertebrate will be useful in characterizing the hematopoietic cell niche and its interactions with hematopoietic cells.

Introduction

The zebrafish, *Danio rerio*, is emerging as a useful model organism for the study of hematopoietic cell transplant (HCT)[42,51]. Its fecundity makes high experimental sample numbers logistically feasible, it is amenable to high-throughput chemical screens for hematopoietic effects of drugs and small molecules, [52] and its optical transparency offers excellent opportunities for direct visualization of cell migration events and *in vivo* fluorescence detection of donor-derived hematopoietic reconstitution. The true extent to which the zebrafish will prove useful for experimental HCT studies, however, will ultimately depend on the degree to which the mechanisms that result in HCT success in mammals are conserved in the zebrafish.

In mammals, the chemokine SDF-1 (CXCL12) and its cognate receptor CXCR4 have been strongly implicated in the homing and reconstitution that occurs during HCT[4,6,53]. SDF-1 is expressed in many organs throughout the body, including the spleen, thymus, skin, heart, lung, kidney, and bone marrow [54, 55]. The widespread anatomical distribution of SDF-1 expression has been shown to play roles in diverse migration and retention events of a wide array of hematopoietic cells, including migration of mast cell precursors in the skin,[56] retention of myeloid cells in extramedullary locations, [57] migration of megakaryocytes in the bone marrow following radiation, [58] migration of hematopoietic stem cells (HSC) to regions of injury, [59] and HSC migration to bone marrow both during homeostasis as well as during HCT [7,10].

In the bone marrow cavity, cells expressing high levels of SDF-1 help to form the HSC niche, and play important roles in hematopoietic stem and progenitor cell (HSPC) support[53]. In addition to high expression of SDF-1, concomitant expression of several cell adhesion molecules and cell surface receptors in the Notch signaling pathway likely contribute to conditions necessary for survival and maintenance of HSCs[60,61]. The exact identity of high SDF-1 secreting cells is unknown but these functions have been ascribed to stromal cells, mesenchymal stem cells (MSCs), perivascular cells, and osteoblasts, all of which have been reported to comprise or contribute to a HSC niche [62,63,64]. Although previous work indicates conservation of some aspects of SDF-1-driven neutrophil hematopoiesis and migration in the zebrafish, [65] the full extent to which the hematopoietic roles of the zebrafish Sdf-1/Cxcr4 axis functionally mirrors that of mammals remains to be seen.

The hematopoietic organ of the adult zebrafish is the kidney, which contains renal tubules interspersed with non-renal stromal cells and hematopoietic stem and progenitor cells (HSPC). Putative HSC of the zebrafish have been found under normal conditions to be located at the surfaces of renal tubules, [66] and putative HSCs of carp have also been reported to home to renal tubules shortly after transplant [67]. While this implies that renal tubule cells form an important component of the adult HSC niche in teleosts, putative HSC niche cells have not been described in the adult zebrafish, nor is it known whether high *sdf-1* expression is a characteristic of the zebrafish HSC niche.

While mammals have a single *sdf-1* gene with multiple splice variants, zebrafish have two *sdf-1* genes; *sdf-1a/(cxcl12a)* and *sdf-1b/(cxcl12b),* which arose from a genome duplication event. *Sdf-1a* and *sdf-1b* share approximately 45% and 47% nucleotide identity, respectively, with the human *sdf-1* gene [68]. The zebrafish *sdf-1a* and *sdf-1b* genes are located on different chromosomes, and share approximately 75% amino acid identity[68,69]. There appears to be some degree of conserved synteny between the human sdf-1 gene (located near the centromere of chromosome 10), and the zebrafish sdf-1a gene (located on chromosome 13), as a few genes located adjacent to sdf-1 on the human chromosome are also represented approximately adjacent to sdf-1a on the zebrafish chromosome.

We report that the anatomical locations of *sdf-1* expression in the zebrafish are similar to those patterns previously reported in mammals. Moreover, *sdf-1* is expressed in high levels in renal tubule cells, which comprise a majority of the marrow in the adult zebrafish, and which may form the HSPC niche. *Sdf-1* is upregulated in a dose-dependent fashion following radiation in the zebrafish, and acts as a chemoattractant to adult zebrafish hematopoietic cells. Because previous studies[68] as well as our own experiments indicated predominant expression of *sdf-1a,* rather than *sdf-1b*, in the teleost hematopoietic tissue specifically, we hypothesized that *sdf-1a* might play a predominate role in recruiting HSPCs. Therefore, we created a transgenic fluorescence reporter of *sdf-1a* expression in order to achieve simultaneous

assessment of donor-derived hematopoietic cell migration and *sdf-1a* expression patterns in HSPC transplant recipients. Using this transgenic reporter, putative hematopoietic niche-defining cells in the kidney were localized as kidney tubule cells. Moreover, *sdf-1a* expressing cells also were found in regions throughout skin of the transplant recipients. Cumulatively, our findings suggest that SDF-1 may guide hematopoietic cell migration following HCT in the adult zebrafish to both medullary and extramedullary sites.

Materials and Methods

Zebrafish Strains and Fish husbandry: Fish were maintained by the University of Minnesota Zebrafish Core Facility according to standardized procedures [70] and with the approval of the International Animal Care and Use Committee, IACUC, University of Minnesota. Wild-type fish were obtained from Segrest Farms (Gibsonton, Florida) and bred in-house. Other fish strains used include AB, *Tg(atp1a1a.4:EGFP)*, [71] *Tg(fli1:EGFP)*, [72] the Casper mutant, [73] and fish carrying the *odysseus* mutation, which consists of a single nucleotide change conferring an early stop codon in *cxcr4b* [74].

Transgenic Construction: The 4.3 kb promoter region of *sdf-1a* was cloned upstream of the *DsRed2* fluorophore in the Tol2 backbone, and injected along with *Tol2* transposase mRNA to facilitate integration, into early zebrafish embryos [75]. Embryos were screened for fluorescence, raised to maturity, and

bred to identify founders. Two independent transgenic lines, each generated from a separate founder fish, were used for this work.

Fish Irradiation: Radiation was delivered through one of the following two systems: (1) With a J.L. Shepherd Mark 1 Model 30 Irradiator, with a Cs^{137} source. Radiation chambers were constructed from petri dishes radially divided with plexiglass into 16 wedge-shaped compartments filled with fish water, each compartment containing a single unanesthetized zebrafish. Radiation chambers were placed on a rotating turntable in front of the source. Fish were irradiated with a single, unfractionated dose at a rate of 6.55 Gy/min. The LD50 identified for this cesium system was 30Gy, and this dose was used for Cesium radiation preconditioning for most transplant experiments. (2) With a X-Rad320 irradiator (Precision X-Ray, Inc.). Unanesthetized fish were placed in a petri dish filled with fish water and placed below the source. Fish were irradiated with a single, unfractionated dose at a rate of 2.7 Gy/min. The LD50 identified for this X-ray system was 20Gy, and this dose was used for X-Ray preconditioning for most transplant experiments. The studies were started with the Cesium based source, but this was decommissioned partway through the experiments. Subsequent studies were performed on the X-ray based source and there were no biological differences found in the ability of the two radiation systems to upregulate *sdf-1* or myeloablate recipients. Kaplan-Meier survival graphs documenting survival

following multiple radiation doses were prepared for each of these radiation delivery methods to determine the LD50 doses (data not shown).

Transplantion: Two days before transplant, transplant recipients were preconditioned with sublethal radiation (specific dose depending on the radiation system as described above). To isolate cells for HCT, donor kidneys were flushed and harvested into Phosphate-Buffered Saline (PBS). Whole kidney marrow (WKM) was isolated by trituration, filtered through a 40 micron filter, and centrifuged at 2000 x g for 6 minutes. For transplant of *odysseus* WKM, vital dye labeling was performed in serum-free, growth-factor free Zebrafish Kidney Stromal Media [45] using CellTracker Green CMFDA (Invitrogen, Carlsbad CA), per the manufacturer's instructions. Supernatant was removed, cells were resuspended in PBS, counted, and kept on ice until transplant. 280,000 dyed WKM cells were transplanted into each recipient via cardiac injections. For myelomonocyte transplants, cells were isolated from WKM via flow-sorting according to FSC/SSC characteristics, counted, and kept on ice before transplant. 100,000 myelomonocytes were transplanted into each recipient.

***In situ* hybridization:** Whole mount in situ hybridization was performed by previously described methods[76]. Tissue was harvested and fixed overnight at 4^0C. in 10% Neutral Buffered Formalin, and dehydrated and stored in methanol at -20°C. Tissues were bleached in 1.5% H_2O_2 for 20 minutes and permeabilized

with 10 µg/ml Proteinase K for 45 minutes at room temperature. Sense and antisense probes labeled with digoxigenin (DIG) were applied at concentrations of 1µg/ml in hybridization buffer, rotated overnight at 55^0C, detected with Anti-DIG-AP Fab fragments, and developed with NBT/BCIP (Roche, Mannheim, Germany) and 1 mM Levamisole. Signal in whole tissues was fixed in 4% paraformaldehyde, rinsed, cleared and photographed in glycerol, then rinsed and soaked overnight at 4^0C in 30% sucrose in PBS, sectioned, conterstained with Nuclear Fast Red (Vector Laboratories Inc. Burlingame, CA), dehydrated in ethanol, cleared in xylenes, and mounted in DPX.

Quantative RT-PCR: Zebrafish were euthanized in tricaine. Fish were beheaded and kidneys were flushed with PBS to remove a large amount of blood from the circulation. For preparation of separate tubule and non-tubule fractions for qRT-PCR, kidneys were harvested into PBS on ice, triturated, and filtered through a 40-micron filter to collect small cells that passed through the filter. These cells were referred to as the “non-tubule” fraction. Tissue failing to pass through the filter (kidney tubules and other stroma) was released from the inverted filter with PBS, and referred to as the kidney tubule fraction. Tubule and non-tubule fractions were then centrifuged at 2000 X g for 5 minutes, PBS was removed, and pellets were frozen in liquid nitrogen. Skin samples were collected by isolating skin from muscle. Total RNA was isolated using Trizol Reagent (Invitrogen) according to guidelines of the manufacturer. cDNA was reverse

transcribed with Superscript III RT-PCR kit (Invitrogen) using random hexamers and qRT-PCR was performed on an Applied Biosystems StepOnePlus, using SYBR green reagent (Invitrogen). Intron-spanning primers were used: sdf-1a (5'cgccattcatgcaccgatttc and 5'ggtgggctgtcagatttccttgtc), sdf-1b (5'cgccttctggagcccagaga and 5'agagattctccgctgtcctcc) and beta-actin (5'gatgcccctcgtgctgtttt and 5'tctctgttggctttgggattca). RQ values were calculated from duplicate reactions for each sample using the delta-delta-Ct method.

In vitro migration assay: Kidneys from large adult wildtype (WT) zebrafish were flushed with PBS, dissected, treated for 5 minutes in 0.0001% bleach in PBS, rinsed several times in PBS, triturated, and filtered through 40 micron filter to isolate HSPC cells. Cells were centrifuged at 2000 X g for 6 minutes, and resuspended in 1:1 DMEM:F12 (Invitrogen) plus 0.5% BSA. Treatment of cells with AMD3100 (Sigma, #A5602) was performed with rotation at room temperature for 2 hours at a drug concentration of 660 μM. Then 3.4 - 3.5 x 10^6 whole kidney marrow cells in 200 μl were loaded into a Transwell® filter basket (5μM pore size, 6.5 mm insert, Costar). Each transwell basket was placed into a culture well containing 500 μl media to which human recombinant SDF-1 (hrSDF-1α) (Calbiochem, #572300) had been added. Cells were allowed to migrate for 2 hrs at 32^0C. Following removal of Transwell® baskets, migrated cells in each culture well were manually counted by a hematocytometer and subjected to flow

cytometry and a uniform flow rate and sample acquisition time period for SSC/FSC analysis.

Immunofluorescence: WKM cell populations were sorted by FSC/SSC characteristics on a BD FACSAria. Sorted cells from each population were blotted onto slides, dried, fixed 20 minutes in methanol at −20^{o}C, blocked in 10% Normal Donkey Serum in DAKO diluent, and stained at a concentration of 1:200 with rabbit polyclonal CXCR4 antibody, cat#PA3-305 (ABR, Golden, CO). Detection of the primary antibody was performed with goat anti-rabbit AF594, cat#A11072 (Invitrogen) at a concentration of 1:400. Negative controls were processed alongside experimentals with omission of the primary antibody.

Statistical analysis: Quantitative data was entered into Prism v5.0 (GraphPad Software, La Jolla, CA). Transplant experiments comparing two groups were analyzed by unpaired two-tailed t-test. For experiments comparing more than two groups, ANOVA analysis with Tukey post analysis was performed, and p values less than 0.05 were identified as significant.

Imaging

Unless otherwise specified, photographs were obtained at room temperature using a DMI series inverted microscope (Leica, Wetzlar, Germany), Retiga 2000R camera (Qimaging, Surrey, BC, Canada), and QCapture acquisition software. Acquisition of brightfield images additionally employed a QImaging

RGB color filter. Live fish were imaged in water, and fresh isolated tissues were imaged in glycerol and PBS. In Adobe Photoshop, fluorescence images were pseudocolored according to the emission of the fluorophore, and pseudocolored photographs of multiple color channels of a single field of view were merged together. Specimens that exceeded a single field of view were documented in several epifluorescence photographs along their length on the x,y plane, and photo montages were assembled manually in Adobe Photoshop. Where sample thickness required it, epifluorescence z-stacks were acquired, processed for deconvolution using MetaMorph, and subsequently merged along the z-axis to produce a single image (Figure 7F).

Quantitative assessment of cell colocalization after HCT

Two days after HCT, kidneys were removed from sacrificed recipient fish, and compressed in glycerol between two coverslips. The entire length of the kidneys were immediately photographed by epifluorescence at a 10× magnification in both the red and green channels. Photo composites of the kidneys in both channels were then assembled manually in Adobe Photoshop CS3. Using the "Select color" tool, the red signal from sdf-1a:DsRed, and the green signal from donor derived cells, was selected and isolated from the rest of the image. Using the "Magnetic Lasso" tool, an outline of each kidney organ was created and given a grey stroke on a new layer. The count tool was used to manually count GFP+ cells that touched DsRed+ cells, and GFP+ cells that did not touch DsRed+ cells. Using the selection tool and the "Record Measurements" function, the total

kidney area within the grey outline, sdf-1a:DsRed-positive area, and sdf-1a:DsRed2-negative area were calculated. The cell co-localization ratios are the percentage of total transplanted cells touching sdf-1a:DsRed-positive tissue divided by the percentage of kidney composed of sdf-1a:DsRed-positive tissue, and the percentage of total transplanted cells located in sdf-1a:DsRed-negative tissue divided by the percentage of kidney composed of sdf-1a:DsRed-negative tissue. A random distribution of cells that fails to preferentially localize to a specific tissue type would give a cell co-localization ratio value of 1.

Results:

***Sdf-1* expression patterns in adult zebrafish:** Due to the paucity of data about the anatomical expression patterns of *sdf-1* in the adult zebrafish, whole mount *in situ* hybridization (WISH) for *sdf-1* expression studies were performed. There are two zebrafish *sdf-1* genes: *sdf-1a* and *sdf-1b,* with unknown, if any, divergence in expression and hematopoietic function in adults. Basal *sdf-1a* and *sdf-1b* expression was seen in adult skin (Figure 1A, E), gills (B, F), and kidney (C-D, G-H). *Sdf-1a* expressing cells in the kidney, the site for hematopoiesis in the zebrafish, included renal epithelial tubular cells and a few vascular-endothelial cells (Figure 1C-D), as well as cells of unknown type interspersed between renal tubules (Figure 2). *Sdf-1b* expression appears strongest in renal tubules, and particularly adjacent to glomeruli (Figure 1G-H). Signal was not seen in controls stained with the sense probe. Thus, *sdf-1a* and *sdf-1b* expression in adult

zebrafish encompass both known sites of hematopoiesis (the kidney) as well as in selected non-hematopoietic organs (the skin and gills), consistent with the possibility that Sdf-1 in adult zebrafish may regulate both medullary and extramedullary hematopoietic cell migration.

Figure 1.

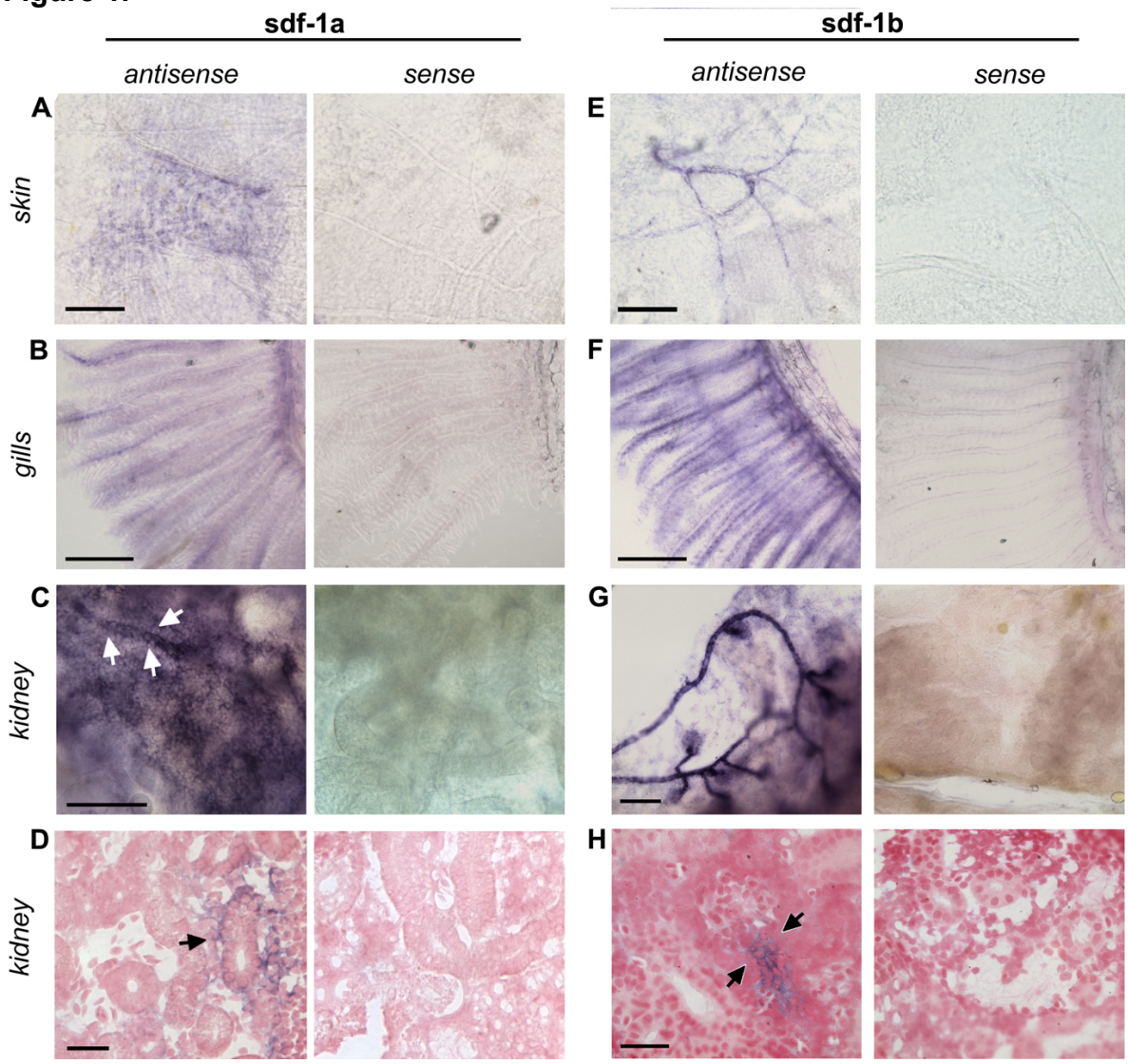

Figure 1. In situ hybridization of zebrafish tissues:

Whole-mount in situ hybridization on tissues from adult zebrafish skin (A, E), gills (B, F), kidney (C-D, G-H). (A) sdf-1a expression in a chevron-shaped pattern in the skin. Bar, 150μM. (E) sdf-1b in skin structures with vascular morphology. Bar,150μM (B) sdf-1a in gills. Bar 250μM. (F) sdf-1b in gills. Bar 250 μM. (C) sdf-1a in the kidney. Arrows indicate kidney tubule. Bar, 100μM. (D) Arrow indicates sdf-1a expression in renal tubules cells. Bar, 25 μM (G) sdf-1b in the kidney, showing strong signal in of glomeruli and adjacent tubules. Bar, 100μM. (H) arrows indicate sdf-1b in proximal renal tubule. Bar, 25 μM.

Figure 2.

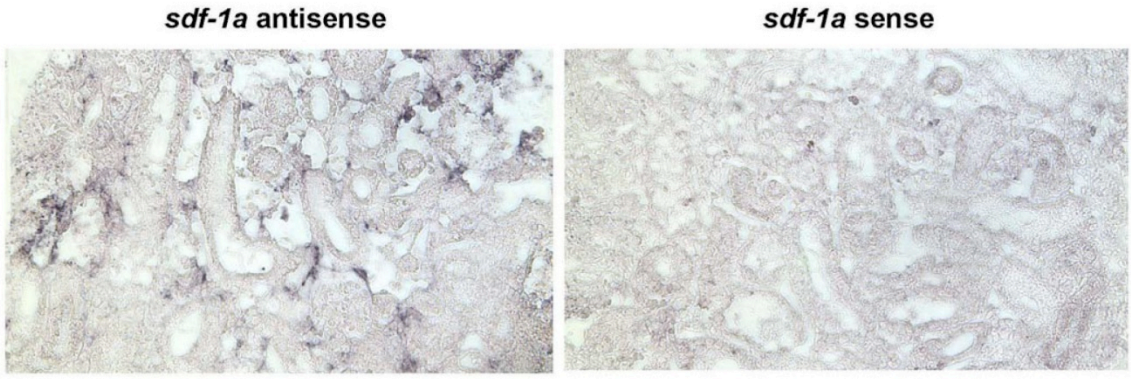

Figure 2. Non-Tubule sites of sdf-1a expression in the kidney:

In situ hybridization of tissue sections of adult zebrafish kidney, DIG-labeled probes.

Radiation-induced upregulation of *sdf-1* in the hematopoietic cell niche of the zebrafish: In mammals, radiation is known to upregulate *sdf-1* expression in the bone marrow compartment, which likely contributes to homing of HSCs and HSPCs to bone marrow [10]. To determine whether *sdf-1* expression is upregulated in the zebrafish marrow in response to radiation, *sdf-1* expression levels were assessed in the kidney following a range of radiation doses. One day post radiation, *sdf-1a* expression in the whole kidney in WT zebrafish increased following radiation by nearly 4-fold when analyzed after 40 Gy as compared to non-irradiated controls; in addition, a dose-response effect was observed at lower radiation doses (Figure 3A).

Since radiation upregulates *sdf-1a* in the kidney, and *sdf-1a* shows expression both in renal tubules and in smaller non-renal cells dispersed between the tubules, we next sought to determine whether the cells responsible

for radiation-induced upregulation of *sdf-1* expression are located in the tubule fraction, or located the non-tubule (HSPC-containing) fraction of the kidney. As *sdf-1* is expressed by the mammalian HSC niche and acts to attract and retain HSCs during hematopoiesis and during HCT, a renal tubule-specific upregulation of *sdf-1* in response to radiation would support the hypothesis that a zebrafish HSC niche is comprised of tubule cells. Trituration and filtration crudely separates the kidney tissue into a 'tubule' fraction enriched for renal tubules and blood vessels, and a fraction composed of smaller cells passing through the filter, which are mostly HSPC. Although sdf-1a expression is present in the non-tubule fraction, we find that radiation-induced increase in both *sdf-1a* and *sdf-1b* expression is most pronounced in the tubule fraction versus the non-tubule fraction one day after radiation (Figure 3B).

Figure 3.

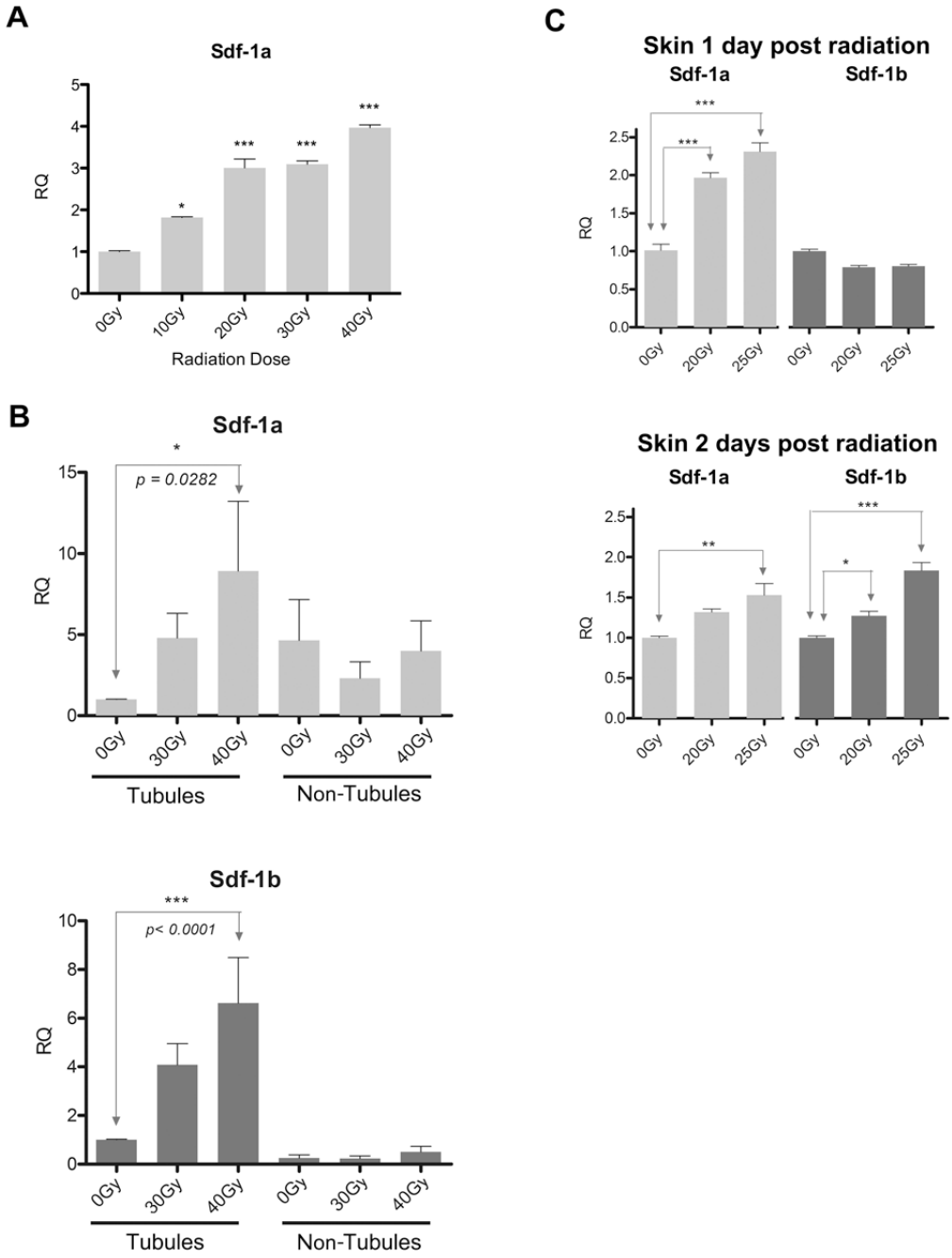
A
Sdf-1a
RQ
Radiation Dose
0Gy
10Gy
20Gy
30Gy
40Gy
B
Sdf-1a
p = 0.0282
Tubules
Non-Tubules
Sdf-1b
p< 0.0001
C
Skin 1 day post radiation
Sdf-1a
Sdf-1b
Skin 2 days post radiation
0Gy
20Gy
25Gy

Figure 3. Sdf-1 upregulation in kidney and skin after pre-conditioning radiation.

(A) qRT-PCR of whole zebrafish kidneys one day after fish received Cs^{137} radiation. n=5 adult fish per group. (B) qRT-PCR of isolated renal tubules fractions and non-tubule fractions one day after fish received Cs^{137} radiation. Data shows pooled results from two independent biological experiments, with an ultimate total of 20-24 fish per condition. (C) qRT-PCR of skin one day (above) and two days (below) after fish received X-ray irradiation. n=skin from 5 fish per condition. (A,B,C) Experimental primers were normalized to B-actin controls. Error bars show mean RQ and SEM between duplicate qRT-PCR reactions. Each radiation group is compared to the 0 Gy reference; *** = $p<.001$., ** = $.001<p<.01$, * = $.01<p<.05$, ANOVA with Tukey post analysis.

Because *Sdf-1* expression has been reported to be upregulated in response to injury in mammalian skin promoting multipotent stem cell migration to injured sites, [77] we hypothesized that radiation exposure could upregulate *sdf-1* expression in zebrafish skin as well. QRT-PCR indeed indicated that radiation-induced upregulation of *sdf-1* expression in the zebrafish is not limited to the kidney, but also occurred in the skin after whole body irradiation of fish (Figure 3C). Both *sdf-1a* and *sdf-1b* were upregulated after irradiation, although *sdf-1a* expression was upregulated by day one, whereas *sdf-1b* upregulation was not evident until the second day post-radiation in the skin. Cumulatively, these findings indicate that radiation causes *sdf-1a* and *sdf-1b* upregulation in the adult zebrafish kidney, predominantly in the renal tubule cell fraction, as well as the skin.

SDF-1 is a chemoattractant for adult zebrafish hematopoietic cells: Having established that radiation increases *sdf-1a* and *sdf-1b* in the putative HSC niche of the zebrafish, we next sought to evaluate the capability of SDF-1 to induce migration of zebrafish hematopoietic cells. Therefore, *in-vitro* migration assays were performed using whole kidney marrow, which contains HSCs and HPSCs, from WT zebrafish. Within two hours, 1 μg/ml concentration of hrSDF-1a induced significant migration (Figure 4).

Figure 4.

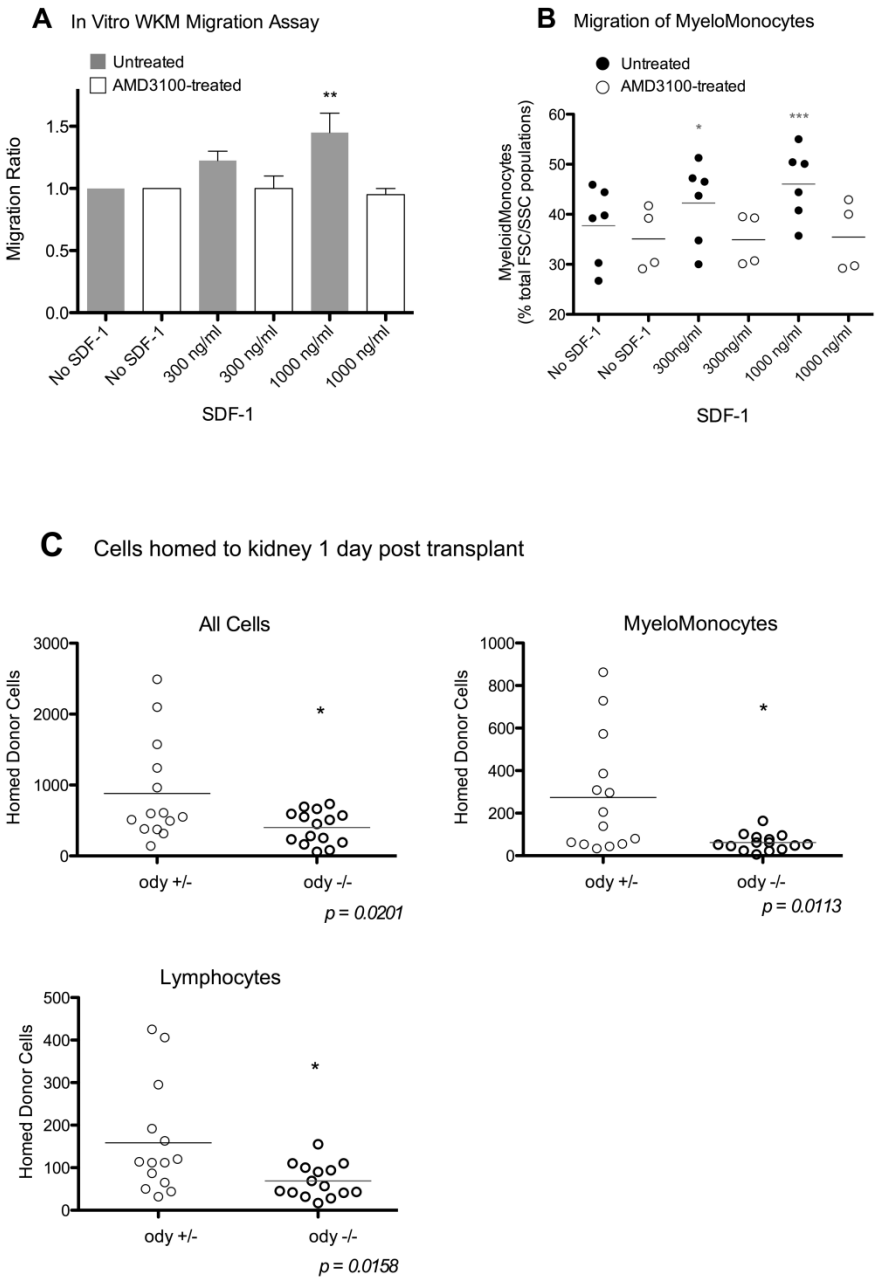
A
In Vitro WKM Migration Assay
Untreated
AMD3100-treated
Migration Ratio
0.0
0.5
1.0
1.5
**
No SDF-1
No SDF-1
300 ng/ml
300 ng/ml
1000 ng/ml
1000 ng/ml
SDF-1
B
Migration of MyeloMonocytes
Untreated
AMD3100-treated
MyeloidMonocytes
(% total FSC/SSC populations)
20
30
40
50
60
*
***
No SDF-1
No SDF-1
300ng/ml
300ng/ml
1000 ng/ml
1000 ng/ml
SDF-1
C
Cells homed to kidney 1 day post transplant
All Cells
Homed Donor Cells
0
1000
2000
3000
*
ody +/-
ody -/-
p = 0.0201
MyeloMonocytes
Homed Donor Cells
0
200
400
600
800
1000
*
ody +/-
ody -/-
p = 0.0113
Lymphocytes
Homed Donor Cells
0
100
200
300
400
500
*
ody +/-
ody -/-
p = 0.0158

Figure 4. SDF-1 chemoattracts zebrafish WKM cells.

(A) 2-hour in vitro transwell migration assay, with migration ratios calculated from hematocytometer total cell counts. Untreated: n=4 experiments, AMD3100-treated: n=2 experiments. Error bars show SEM. (B) FACS analysis of migrated cells from in vitro migration assays. Percent myelomonocytes are calculated from a cell population with FSC/SSC properties of lymphocytes, precursors, and myelomonocytes. Bars show the mean. Untreated: n=4 experiments, AMD3100-treated: n=3 experiments. *** = p<.001., ** = .001<p<.01, * =.01<p<.05, ANOVA with Tukey post analysis. (C) *Odysseus* mutant WKM was labeled with vital dye and transplanted into AB and WT fish preconditioned with 20Gy X-ray irradiation. Recipient kidneys were harvested and analyzed by flow cytometry one day post transplant. Graphs show the number of donor-derived cells detected per 60,000 total cells. Bars show the mean. n=2 experiments, unpaired t-test.

Flow cytometry analysis of migrated cells revealed that myelomonocytes were the predominant cell type migrating towards hrSDF-1 and that such migration occurred in an hrSDF-1 concentration-dependent fashion (Figure 4B). This migration was blocked by pre-treatment of WKM cells with AMD3100, a chemical antagonist that blocks the CXCR4:SDF-1 interaction, used at a concentration of 660 μM, the maximum concentration that did not increase apoptosis of WKM cells as compared to non-treated controls. Migration of other cell populations (lymphocytes and precursors) showed no significant increase in migration with the addition of hrSDF-1 (data not shown).

These *in vitro* studies showing that SDF-1 induces migration of zebrafish hematopoietic cells, combined with our finding of radiation-induced *sdf-1*

upregulation in hematopoietic tissue, suggested that endogenous Sdf-1 directs hematopoietic cell homing *in vivo* in irradiated adult zebrafish during HCT. To determine whether *in vivo* administration of AMD3100 could be used to inhibit HSPC homing similar to the *in vitro* effect we observed, we performed HCT with WKM cells pre-treated for two hours with 660 μM AMD3100. In three independent trials, impairment of homing was subtle and subsequent experiments with different cell doses and different genetic backgrounds failed to confirm these initial results (data not shown).

In other studies we attempted to use AMD3100 as a mobilizing agent. We found no changes in HSPC mobilization in fish treated with AMD3100 (data not shown). Future experiments examining different doses and schedules of AMD3100 would be required to reach a conclusion as to whether AMD3100 has the capacity in zebrafish to block Sdf-1:Cxcr4 binding *in vivo*.

In order to further assess the possibility that Sdf-1:Cxcr4 interaction regulates the homing of WKM cells *in vivo*, we took advantage of a zebrafish line, *odysseus*, in which one of the two *cxcr4* genes is mutated (*cxcr4b* specifically) [74]. We performed HCT using donor hematopoietic (WKM) cells obtained from the adult *odysseus* and found that transplants of homozygous *odysseus* mutant hematopoietic cells resulted in significantly fewer homed cells in the WT recipient kidney than transplants of heterozygous mutant hematopoietic cells (Figure 4C). The homing of lymphoid and myelomonocytic lineage cells were reduced when homozygous *odysseus* vs heterozygous WKM cells were infused. These data

indicated that the Sdf-1/Cxcr4 axis is important in zebrafish hematopoietic cell homing as is the case in mammals.

To confirm Sdf-1 protein expression in WKM cells, CXCR4 immunofluorescence staining of WKM populations sorted according to FSC/SSC properties was performed. Cells expressing CXCR4 were present in all three cell populations. Qualitatively, the greatest prevalence of CXCR4-positive cells resided in the myelomonocyte population (Figure 5) as would be predicted by the results of the in vitro WKM migration assay.

Figure 5.

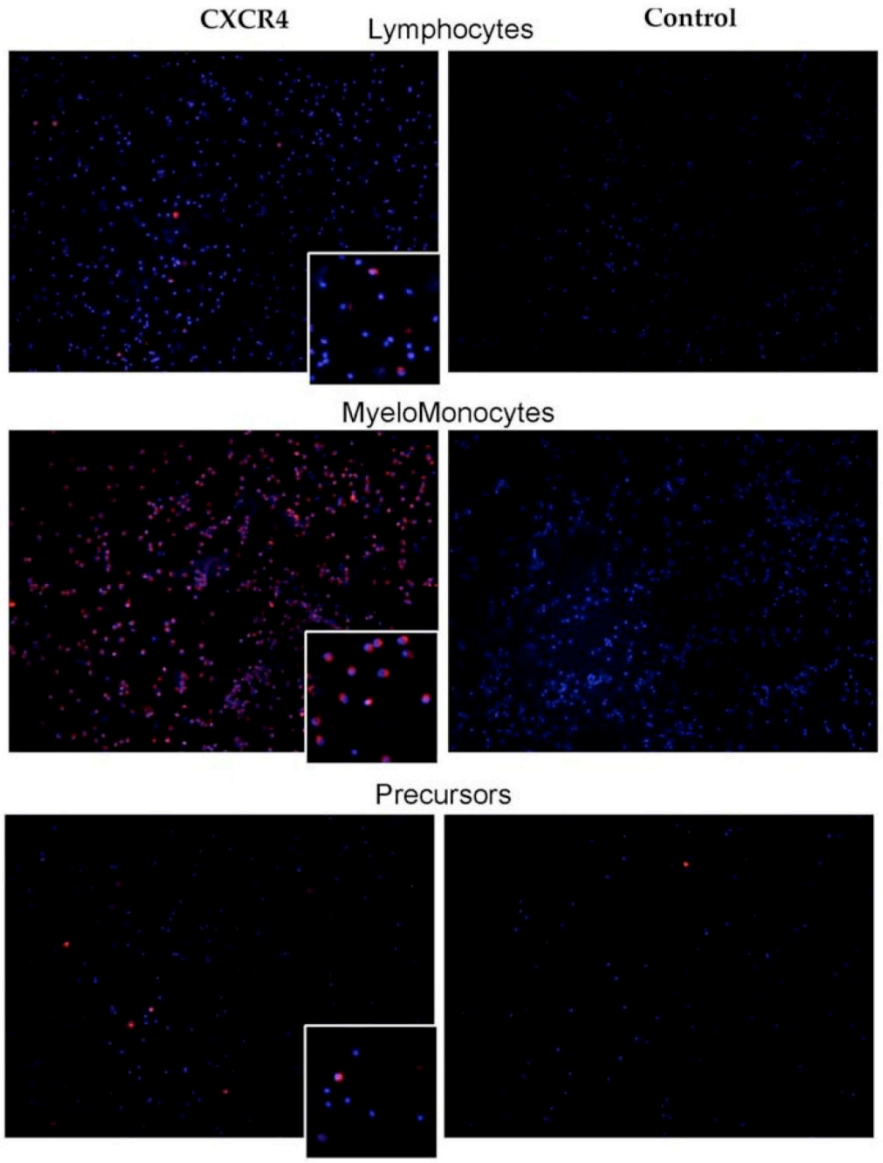

Figure 5: Zebrafish hematopoietic cells express CXCR4

Lymphocytes, MyeloMonocytes and Precursors were stained for CXCR4 (red) and dapi (blue). All three populations contained positive cells, but MyeloMonocyte cells showed the most positivity.

Localization of *sdf-1a* expression in adult transgenic zebrafish.

Both in situ hybridization (Figure 1) and QRT-PCR analysis of WT zebrafish organs (Figure 6) indicated greater constitutive expression of *sdf-1a* in the adult zebrafish kidney than *sdf-1b*.

Figure 6.

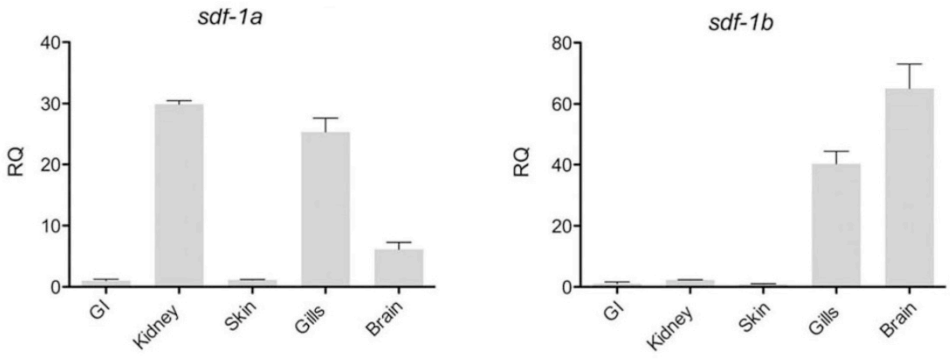

Figure 6: Constitutive *sdf-1* expression in adult zebrafish organs:

Expression of *sdf-1a* and *sdf-1b* was determined through qRT-PCR analysis of organs. Gastro-Intestinal tract (GI) was selected as the reference organ, and Beta-actin used as the control. Each sample was composed of organs from five adult WT fish. Error bars indicate standard deviations for 2–3 reactions.

To more precisely analyze cells that define the putative hematopoietic cell niche in zebrafish, we decided to generate *sdf-1a* transgenic zebrafish that contained the *sdf-1a* promoter linked to a reporter fluorophore, *DsRed2*. The resulting transgenic line permits *in vivo* fluorescent detection of *sdf-1a* promoter activity, which mirrors that of the endogenous promoter. For this purpose, the 4.3 kb promoter region of sdf-1a was cloned upstream of the *DsRed2* fluorophore in the Tol2 backbone and injected into early zebrafish embryos along with *Tol2*

transposase mRNA to facilitate integration. Two independent lines of *Tg(sdf-1a:DsRed2)* with similar expression patterns were utilized, each generated from a different founder fish. The use of *Tg(sdf-1a:DsRed2)* zebrafish avoids the technical issues of fixation and processing that is required for WISH, and also facilitates flow cytometry based analysis and isolation. In the *Tg(sdf-1a:DsRed2), sdf-1a* expression in the intact organism is readily visualized in the skin in chevron-shaped structures, and gills (Figure 7A-B) as well as in renal tubules (Figure 7C-F), mirroring the mRNA expression patterns observed by WISH. Sdf-1a expression is also reported in pericytes (Figure 7G).

Figure 7.

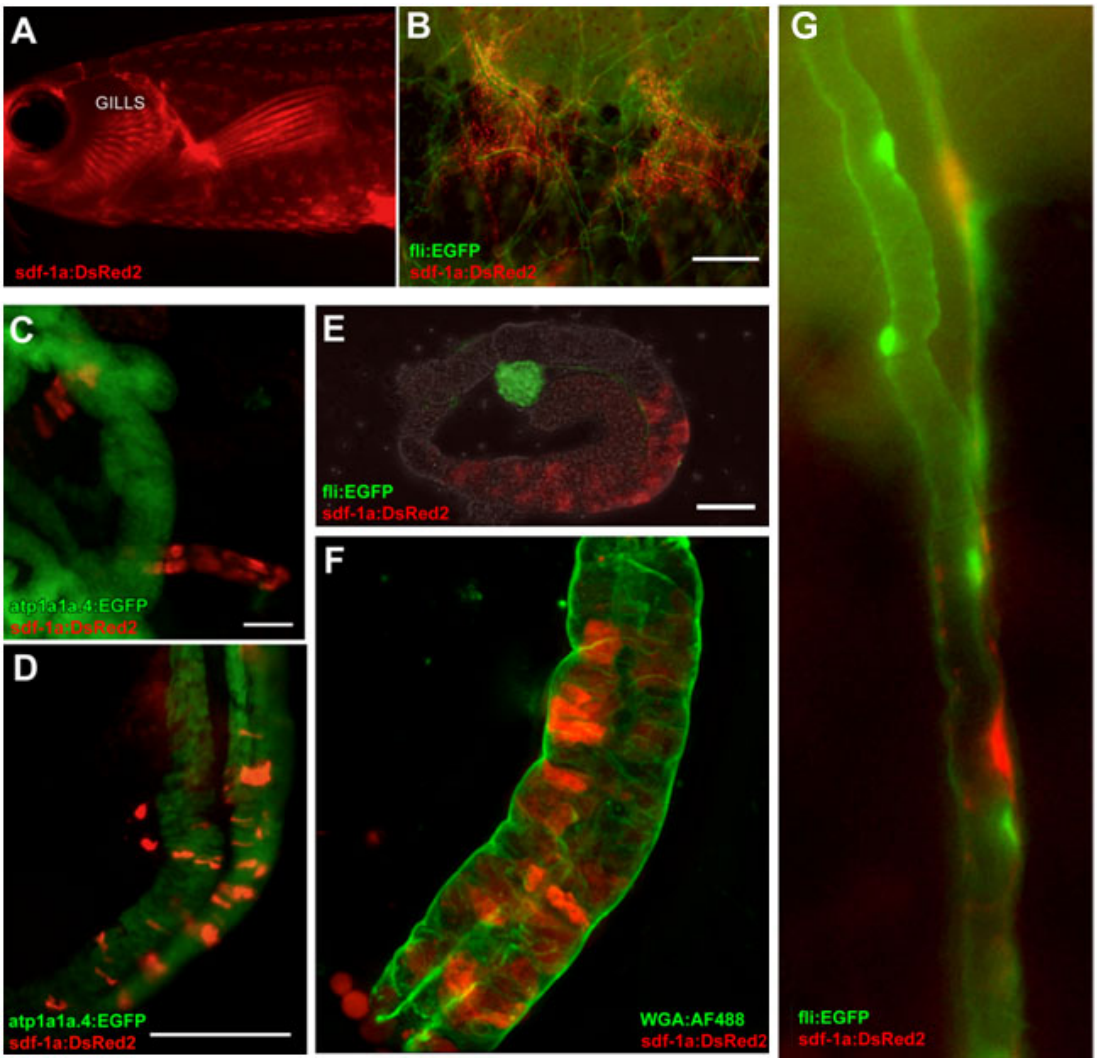
A
GILLS
sdf-1a:DsRed2
B
fli:EGFP
sdf-1a:DsRed2
G
fli:EGFP
sdf-1a:DsRed2
C
atp1a1a.4:EGFP
sdf-1a:DsRed2
E
fli:EGFP
sdf-1a:DsRed2
D
atp1a1a.4:EGFP
sdf-1a:DsRed2
F
WGA:AF488
sdf-1a:DsRed2

Figure 7. Sdf-1a expression reported by *Tg(sdf-1a:DsRed2).*

(A) *In vivo* fluorescence signal reporting *sdf-1a* expression in the adult transgenic, revealing expression in the skin and gills. (imaged with a Leica MZ FLIII fluorescence stereomicroscope) (B) *in vivo sdf-1a:DsRed2* (red) indicates *sdf-1a* expression in chevron-shaped structures in the skin, and fli:EGFP (green) expression marks vessels in a double transgenic fish with both reporters. Bar, 200μM. (C) *Sdf-1a:DsRed2* expression in renal tubules that do not report expression of *atp1a1a.4*, in a fish transgenic for both reporters. Bar, 50μM. (D) *Sdf-1a:DsRed2* expression in distal renal tubules that also express *atp1a1a.4*, in a fish transgenic for both reporters. Bar, 125 μM. (E) *fli:EGFP* expression marking vessels of a glomerulus, and *sdf-1aDsRed2* expression in an immediately adjacent (proximal) renal tubule of a transgenic fish with both reporters, imaged in PBS. Bar, 50μM. (F) An isolated kidney tubule showing *sdf-1a:DsRed2* signal in renal tubule cells. Green: WGA-AF488 applied to fresh tubules at 10μg/ml for 20 minutes on ice (a concentration calculated to produce widespread nonspecific labeling for purposes of revealing basic tubule morphology). After staining specimen was rinsed in PBS and immediately imaged in glycerol compressed between two glass coverslips, using a 40X oil-immersion objective. (G) *Sdf-1a:DsRed2* expression is seen in pericytes along fli:EGFP capillaries, in fish transgenic for both reporters.

To better define the relationship between *sdf-1a* expression and blood vessels, the *Tg(sdf-1:Dsred2)* was mated with a *fli-1:EGFP* transgenic zebrafish. The transcription factor *fli-1* is expressed in all vessels and hence the blood vasculature in *fli-1:EGFP* transgenics is GFP positive. We find that chevron-shaped sites of *sdf-1a* expression in the skin exist almost exclusively in regions of high concentrations of *fli-1*$^{+}$ blood vessels, which form islands of vascular plexuses distributed across the body of the fish in a pattern that mirrors the distribution of the fish scales (Figure 7A-B).

In order to clarify the nature of the tubules containing cells expressing sdf-1a, *Tg(sdf-1a:DsRed2)* was crossed to *Tg(atp1a1a.4:EGFP),* which labels distal tubules and collecting ducts within the adult kidney (Iain Drummond, personal communication, Aug. 3, 2009). Examination of the double transgenic adult zebrafish kidney revealed co-localization of *sdf-1a* and *atp1a1a.4*-negative renal tubules (Figure 7C), as well *sdf-1a* expression in *atp1a1a.4:EGFP*-positive renal tubules (Figure 7D). *Sdf-1a:DsRed2*-expressing kidney tubules are also found located adjacent to glomeruli (Figure 7E). Taken together, these data indicate that cells with high *sdf-1a* expression are present in proximal tubules as well as distal tubules or collecting ducts.

Hematopoietic cells migrate in vivo toward sites of sdf-1 expression in zebrafish after radiation and HCT: *Tg(sdf-1a:DsRed2)* were assessed by microscopy to determine whether transplanted hematopoietic cells homed to regions of high *sdf-1a* expression in the zebrafish in the context of HCT. Three days after WKM transplants in irradiated recipients, GFP-positive donor-derived cells can be found localized to the regions of the skin that showed DsRed2 expression (Figure 8B). Two days after transplanting a fraction of WKM cells enriched for the myelomonocyte lineage, fluorescent donor-derived cells were found distributed throughout the kidney, with some transplanted cells found immediately adjacent to tubule cells expressing dsRed (Figure 8A). Analysis of three recipient fish in the same experiment indicated donor derived cells were localized with a significantly higher frequency to regions of sdf-1a:DsRed signal in the recipient kidney than would be expected of random distribution (Figure 9). Consistent with *in vitro* data and transplant experiments demonstrating the migration of hematopoietic cells to Sdf-1, exposure of the zebrafish to radiation upregulated *sdf-1* in the adult zebrafish kidney, the putative HSC niche, and hematopoietic cells indeed migrated to sites of high *sdf-1a* expression in the kidney and skin.

Figure 8.

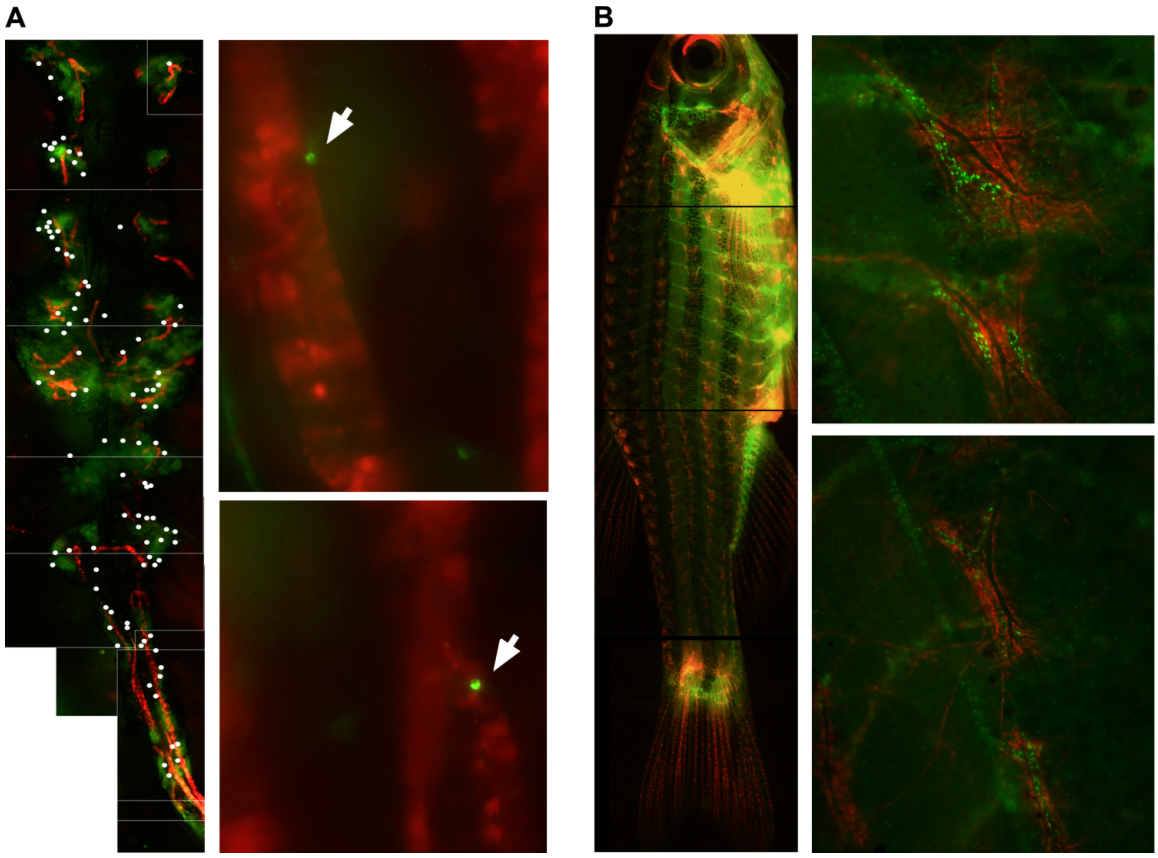

Figure 8. After HCT, donor cells migrate to sdf-1a:DsRed2 structures in recipients.

(A) Photo composite of images taken with a 10X/0.3 NA objective of an *ex vivo* kidney of *Tg(sdf-1a:DsRed2)* four days after preconditioning with 30 Gy Cesium radiation and two days after transplant with 100,000 Green Glofish MyeloMonocyte cells. For clarity, locations of donor-derived GFP^+ cells are marked with a white dot (left panel). GFP^+ donor-derived cells can be found adjacent to sdf-1a:$DsRed2^+$ tubules. Photos taken with a 40X/0.6 NA objective. (right panels). (B) Photo composite of a *Tg(sdf-1a:DsRed2)* fish five days after preconditioning with 25Gy X-ray radiation and three days after transplant with $1x10^6$ Green Glofish WKM cells. Photos taken with a Leica M165 FC fluorescent microscope, Planapo 1.6x/.05 NA objective, Leica DFC340 FX camera and Leica Application Suite software. (left), and detail of regions of concentrated localizations of *sdf-1a:dsRed* cells and GFP^+ donor-derived cells. Photos taken with a 10X/0.3 NA objective and IP Lab acquisition software (right).

Figure 9.

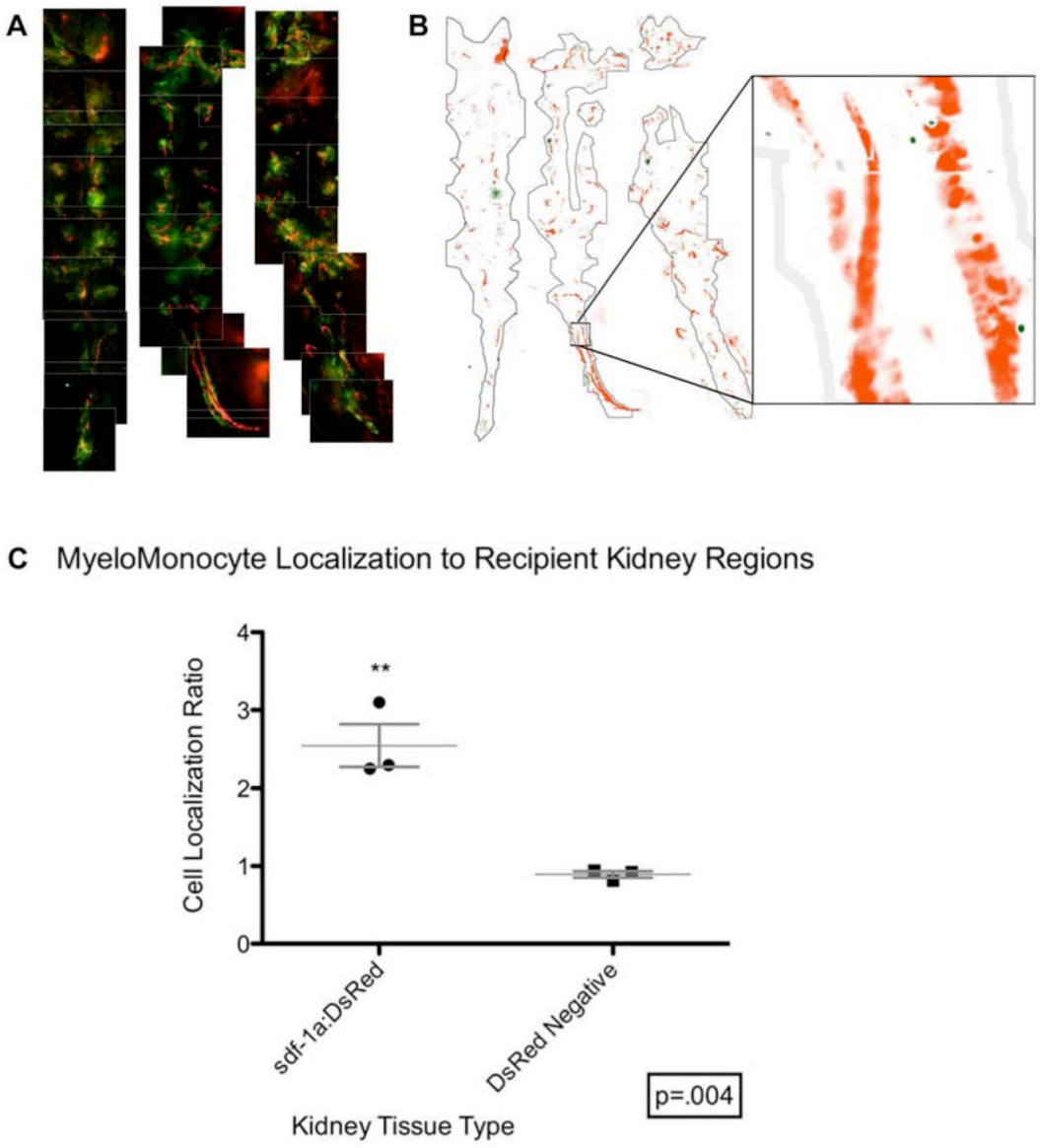

Figure 9: Quantitative assessment of cell colocalization after HCT

Two days after HCT kidneys were photographed (A), and the GFP signal, DsRed signal, and outline of each kidney organ were digitally isolated (B). The cell co-localization ratios were calculated from information in previous panels (C). Each data point in the plot represents calculations from the entire kidney of one fish, as shown in panels A and B. Significance was assessed by a two-tailed t-test.

Discussion

SDF-1 orchestrates several hematopoietic cell migration and retention events in mammals, both during homeostasis as well as during HCT and hematopoietic reconstitution. It is a chemoattractant for several hematopoietic cell types, including HSPCs, leukocytes, and granulocytes, upregulated in response to radiation-induced tissue damage, expressed in several locations throughout the organism, and present at high levels in the HSC niche in the bone marrow[78]. Our data reveal that Sdf-1 in the adult zebrafish has functional similarities to mammals in its upregulation in response to radiation, capacity to induce hematopoietic cell migration *in vitro* as well as *in vivo*, anatomical expression patterns in extramedullary sites throughout the organism, and high expression levels in putative HSC niche cells, which in the zebrafish include kidney tubular epithelial cells. Together, these data provide support for the use of zebrafish to study HSC and HSPC migration after radiation and HCT, allowing visualization of the homing pattern in the whole organism.

In the adult zebrafish, reagents for refined hematopoietic identification of specific cell populations such as HSCs are still in development. Nonetheless, our findings that zebrafish cells of myeloid characteristics show significant *in vitro* migration toward SDF-1, which can be inhibited by an AMD3100 blockade of Cxcr4, bear similarity to previous reports of migration of mammalian hematopoietic and effector cells toward SDF-1[32,79]. This indicates that the capacity of Sdf-1 to induce hematopoietic cell migration is conserved in the adult

zebrafish. Although we were unable to document an effect of AMD3100 administration *in vivo* on homing of WKM cells during HCT or mobilization of WKM cells in non-transplanted zebrafish, which we hypothesize is due to the lack of information as to the optimal dose and schedule of the drug, our observation that donor-derived WKM cells and myelomonocytes co-localize with sdf-1a:DsRed positive cells in the skin and kidney following HCT is compatible with the conclusion that endogenous Sdf-1 acts as a bona fide hematopoietic chemoattractant in the zebrafish *in vivo* during HCT.

Data generated using WISH, qRT-PCR, and the *Tg(sdf-1a:DsRed2)* reporter line indicate that some renal tubule cells express high levels of *sdf-1*. Furthermore, radiation-induced upregulation of *sdf-1* in the hematopoietic organ occurs in kidney tissue fractions enriched for renal tubules. Investigators have proposed that radiation-induced *sdf-1* upregulation specifically in "niche" cells of the bone marrow induces HSC homing to the niche following HCT [80,81]. Previous suggestions in the literature indicate that the putative HSC niche of the zebrafish may be comprised of renal tubule cells[66, 67]. These reports, combined with our findings here that renal tubule cells express high levels of *sdf-1* and upregulate expression in response to radiation, cumulatively indicate that *sdf-1* may be a hallmark of a zebrafish HSC niche located on the renal tubules.

Further, our findings regarding *sdf-1* expression in the whole organism have implications for extramedullary HSPC migration in mammals. Although SDF-1 expression has been reported previously in the human skin, [55] our

observation of WKM migration to concentrated regions of constitutively expressed *sdf-1* in the zebrafish skin suggests the possibility of a dermal or epidermal structure that could act as an attractant or niche for stem or progenitor cells. Alternatively, CXCR4 expressing cells recruited to the skin may not be indicative of extramedullary hematopoiesis but instead may play a role in controlling inflammatory responses in the skin that occur following whole body irradiation.

Although the mature mammalian human kidney is not generally regarded to be a hematopoietic organ, it has been reported capable of supporting hematopoiesis[82]. The presence of a renal tubule HSPC niche in the zebrafish raises the intriguing question of whether mammalian renal tubule cells retain some functions in stem cell attraction and maintenance. The fact that renal tubule expression of SDF-1 has also been reported in humans, mice, and rats suggests a conservation of useful biological functions carried out by SDF-1 at this location. Indeed, SDF-1 expression by renal tubules has been strongly implicated in inducing cell migration and repair processes in the context of renal injury [83-85]. Conversely, there are several reported characteristics of the mammalian HSC niche, such as high levels of SCF and ALCAM expression,[4,61] as well as expression of adrenergic receptors and potential participation in neuroreticular complexes,[7] which have yet to be characterized in this putative HSC niche of adult zebrafish. It remains to be seen whether the HSC niche in the adult zebrafish kidney shows similarity to the mammalian HSC niche with regards to

broader gene expression profiles and physical proximity to other cell types or complexes that might contribute to HSC maintenance.

In summary, we have generated a *sdf-1a:DsRed2* transgenic zebrafish that facilitates the identification of the HSC niche, likely to be renal tubule cells in the adult zebrafish. Moreover, our results indicate that in the adult zebrafish, Sdf-1 has similar roles in HSC attraction and support as it does in mammals. Although conclusive functional evidence of this will await the refinement of methods for the identification and isolation of HSCs in the adult zebrafish, the newly generated *sdf-1a:Dsred2* transgenic line will permit flow cytometry isolation of putatitve cells in the HSC niche in the zebrafish that may recruit donor HSCs and HSPCs and support zebrafish hematopoiesis in the resting as well as perturbed state that accompanies radiation and HCT.

Acknowledgments:

The authors thank the University of Minnesota Zebrafish Core Facility for fish maintenance and breeding assistance. Assistance in cell sorting was provided by the Flow Cytometry Core Facility of the Masonic Cancer Center. Thanks to Ian Drummond for providing the Tg(atp1*a1a.4:EGFP*) fish, and for valuable discussion and insight. Thanks to Jamie Van Berkum and Todd Smith for microscopy assistance. Thanks to Paul Stadem for assistance in sample preparations. This work was supported in part by funding from a graduate student fellowship provided by the 3M Corporation (T.J.G.)

Chapter 3:
Effect of Radiation Dose-Rate on the Adult Zebrafish Model of Hematopoietic Cell Transplant

Foreword

Although exceptionally high radiation dose-rates are currently attaining clinical feasibility, there have been relatively few studies reporting the biological consequences of these dose-rates in hematopoietic cell transplant (HCT). In zebrafish models of HCT, preconditioning before transplant is typically achieved through radiation alone. We report the comparison of outcomes in adult zebrafish irradiated with 20Gy at either 25 or 800 cGy/min in the context of experimental HCT. In non-transplanted irradiated fish we observed no significant differences between dose-rate groups as assessed by fish mortality, cell death in the kidney, endogenous hematopoietic reconstitution, or gene expression levels of *p53* and *ddb2* in the hematopoietic and renal kidney. However, following HCT, recipients conditioned with the higher dose rate showed significantly improved donor-derived engraftment at 9 days post transplant ($p \leq 0.0001$). Analysis for *sdf-1a* expression, as well as transplant of hematopoietic cells from *cxcr4b -/-* zebrafish, *odysseus,* cumulatively suggest that the *sdf-1a/cxcr4b* axis is not required of donor-derived cells for the observed dose-rate effect on engraftment. Overall, the adult zebrafish model of HCT suggests that exceptionally high radiation dose-rates can impact HCT outcome, and offers a new system for radiobiological and mechanistic interrogation of this phenomenon.

Key words: Radiation dose rate, Total Marrow Irradiation (TMI), Total body irradiation (TBI), SDF-1, Zebrafish, hematopoietic cell transplant.

Introduction

Radiation preconditioning is often used to prepare patients for Hematopoietic Cell Transplant (HCT), and is also a common preconditioning method in animal models used to study the mechanisms of hematopoietic cell homing and engraftment. Radiation dose-rates for clinical preconditioning total body irradiation (TBI) commonly range from 5-30 cGy/min [86]. However, clinical feasibility and efficacy have recently been demonstrated for alternative radiation delivery methods capable of markedly higher dose rates, up to 800 cGy/min [87,88]. Although these higher radiation dose-rates have been shown to be compatible with hematopoietic engraftment in humans, it is unknown whether they can have unique impacts on the marrow microenvironment or kinetics of hematopoietic engraftment.

Historically, studies comparing effects of radiation dose-rate for TBI at ranges substantially lower than 800 cGy/min found strong correlations between higher dose-rates and non-hematopoietic toxicity, with dose-rate effects on hematopoietic damage observed to be less striking than the adverse dose-rate effects on organs such as lung and gastrointestinal tract [89,90]. However, despite reductions in off-target toxicities associated with lowered dose-rates, prohibitively longer delivery times required to deliver a desired dose at a low rate during a single treatment session could present logistical drawbacks [91]. Early recognition of this dilemma helped to promote fractionated delivery, with goals to minimize organ toxicity, while leaving hematopoietic ablation effects essentially intact [91].

Today new advances in conformal radiation now allow exceptionally high dose-rates targeted to the bone marrow alone, while sparing non-target organs [92]. This makes it possible to consider the therapeutic outcomes of high dose-rates that were traditionally considered inadvisable, and prompts renewed interest in refining our understanding of radiation dose-rate effects as they relate specifically to HCT and engraftment.

Anticipating the consequences of increasing radiation dose-rates in a biological process as complex as HCT is not necessarily straightforward. Inverse correlations have been reported between dose-rate and the dose required for engraftment after HCT. In murine models comparing dose-rate ranges at and below 50 cGy/min, this effect has been attributed to the capacity of the higher dose-rates to cause greater lethality to recipient proliferating T-lymphocyte precursors [93,94]. However, improved engraftment caused by higher dose-rates has been reported to occur in syngenic transplants as well [93], raising the possibility of unknown alternative mechanisms enforcing this dose-rate dependent outcome. Additionally, although it seems reasonable to expect greater recipient cell lethality after higher dose rates, there are some experimental contexts in which moderately higher dose-rates actually cause significantly less irradiated cell lethality than very low dose-rates, arguably due to more efficient DNA damage detection and repair responses elicited by higher rates of damage [95].

Transplant of adult zebrafish can be used to experimentally model HCT. The primary hematopoietic organ in the zebrafish is the kidney, and the use of radiation to precondition adult zebrafish for HCT of donor hematopoietic cells obtained from the kidney is well established [73,96,97]. Zebrafish show evidence for conservation of mammalian DNA damage recognition and repair mechanisms, including those dependent on p53, and can additionally be used to screen for chemical modifiers of radiation sensitivity [40,41,98,99]. However, little is known about the impact of different radiation dose rates on this vertebrate model. In this study, we compared adult zebrafish preconditioned with 20 Gy delivered with dose-rates of either 25 cGy/min, or 800 cGy/min, to determine the impacts, if any, of the dose-rates on this experimental system. Although indicators of radiation-induced toxicity in the kidney were observed to be similar in both the 800 cGy/min and 25 cGy/min dose-rate conditions, we found that recipients irradiated at the higher dose rate showed significantly greater levels of donor-derived cells 9 days post transplant (dpt), compared to recipients irradiated at the lower dose rate.

Materials and Methods

Zebrafish care: Adult wild type (WT), transgenic Tg(*bactin2:EGFP*) [100], Tg(*h2afv:eGFP*) [101] , Tg(*sdf-1a:DsRed*) [97], and *odysseus* mutant [50] zebrafish were housed in the University of Minnesota Zebrafish Core Facility according to previously described standards of care [102] . Fish used in this study were raised to a

minimum age of two months. The methods used in this work were approved by the *Institutional Animal Care and Use Committee* (*IACUC*), University of Minnesota.

Radiation Delivery to Zebrafish: All experiments reported here used a total dose of 20 Gy, and dose rates of either 25 cGy/min, or 800 cGy/min, to irradiate adult zebrafish in fish water within a large petri dish. For all radiation sessions, the petri dish was placed on 5 cm thick solid water material to prevent scattering. A 1.5 cm thick tissue-equivalent bolus material to accommodate dose build up and ensure accurate dose delivery to the spatial location of the zebrafish was placed on top of the petri dish. Dose was delivered with a Varian 2300CD linear accelerator (Varian, CA). The inverse square relation were used to determine the correct SSD for the desired dose rates based on the dose rate delivered at 100 SSD.

For radiation delivery at the 25 cGy/min dose rate, we used a surface to source distance (SSD) of 200 cm between the source and the surface of the bolus. The linac was programmed to deliver 100 cGy/min at 100 SSD (by setting 100 monitor unit or MU/minute). This achieved a dose rate of 25 cGy/min. For radiation delivery at dose rate of 800 cGy/min, surface to source distance (SSD) was kept at 87 cm between the source and the bolus, and the linac was programmed to deliver 600 cGy/min at 100 SSD. This achieved a dose rate of 800 cGy/min.

Dose verification and dose rate verification: Dose rates were verified with routinely used in-house Ionization chamber [PTW, TN30013] and an electrometer [Keithley 602]. The dose homogeneity across the petri dish, measured using the extended dose rate (EDR) film, was observed to be within 5%. The ionization chamber was placed within solid water material, positioned 5mm below the petri-dish.

For the high dose rate (800 cGy/min), the dose rate was measured to be 0.217 x 10^{-8} Ampere (varied between 0.216 to 0.218), and the total beam on time was 2.5 minutes. For the low dose rate (25 cGy/min), the dose rate was measured to be 0.68 x 10^{-10} Ampere (varies between 0.660 to 0.704), and the total beam on time was 82.1 minutes. The dose rate ratio measured using electrometer reading between high dose and low dose rate delivery was $0.217 \times 10^{-8} / 0.68 \times 10^{-10}$ = 31.9. This is equivalent to the expected dose rate ratio of 32 (800/25), i.e., the time required to deliver the low dose rate irradiation was 32 times greater than the time required to deliver the high dose rate irradiation.

Hematopoietic cell transplantation (HCT): Two days following irradiation, HCT was performed by previously described methods [96]. Briefly, donor fish were euthanized in tricaine, beheaded, flushed with PBS, and kidneys were removed into sterile 1X DPBS. Kidneys were triturated, and filtered through a 40 uM filter to isolate whole kidney marrow cells (WKM). WKM cells were pelleted,

resuspended in Phosphate Buffered Saline (PBS), counted, and transplanted into anesthetized recipient fish through cardiac injection. Each recipient fish received a transplant cell dose of 400,000 WKM cells.

Hematopoietic cell analysis: Viability of WKM cells was determined by staining with Propidium Iodide (BD Phamingen) and analyzed by flow cytometry, using a BD FacsCanto. Hematopoietic cells (myelomonocytes, lymphocytes, precursors) were identified through FSC/SSC characteristics as previously described [96], and donor-derived hematopoietic cells were identified through GFP expression. 100,000 to 250,000 events were collected per sample, with numbers of total collected events the same for all samples within an experiment.

qRT-PCR of zebrafish tissues: Isolation of WKM and renal tubules from zebrafish kidneys was performed as described previously [97]. RNA isolation and DNA removal were achieved through RNeasy Mini Kit (Qiagen). cDNA was synthesized using SuperScript III 1st strand synthesis kit (Invitrogen). qRT-PCR was performed using either SYBR green reagents with previously reported intron-spanning primers to *bactin1, sdf-1a* and *sdf-1b* [97] or Taqman Primers and reagents (Applied Biosystems) for *bactin1* (Dr03432610_m1), *ddb2* (Dr03429615_m1) and *p53* (Dr03112089_m1). qRT-PCR reactions were performed in technical triplicates on a StepOnePlus qRT-PCR system (Applied

Biosystems). Each biological sample analyzed by qRT-PCR was composed of tissues pooled from 4-5 fish.

Microphotography and Image Analysis: Single-channel photographs were acquired using Leica LAS software, DFC340FX camera, and Leica MZ6 stereomicroscope, and Leica GFP filter cube. Specimens too large to fit within a single field of view were photographed across the xy plane as needed, and photomontages were manually assembled in Adobe Photoshop CS4. Where indicated, quantitative assessment of Green Fluorescent Protein (GFP) signal was accomplished using one photo composite of each fish, cropped to isolate the body only, and analyzed for the mean gray value in ImageJ. Dual-channel photographs were obtained using a DMI6000B Leica microscope, Retiga2000R camera, and QCapture Basic acquisition software. Adobe Photoshop CS4 was used to pseudocolor and assemble photo composites.

Results

Effects of Dose Rates on Zebrafish Survival and Myelosuppression: In order to compare the relative impacts of 25 cGy/min and 800 cGy/min dose-rates on fish irradiated with 20 Gy, we performed survival, cell death, and myelosuppression studies on irradiated, non-transplanted adult WT zebrafish. Two independent trials, each composed of 10 fish per group, revealed no significant differences between dose rate groups in survival over 20 days (Figure 1A). TUNEL staining and H&E in kidney sections one day after radiation

suggested similar levels of apoptosis and hematopoietic cell loss, respectively, in both dose rate groups (Figure 1B). Flow cytometry analysis of WKM isolated from WT fish at multiple time points following radiation revealed hematopoietic cell loss and subsequent recovery, as has been previously reported to occur following sublethal irradiation of fish [96]. However, there were no significant differences between dose-rate groups in the relative numbers of viable hematopoietic cells present in the kidney during this endogenous reconstitution process. Although some fish irradiated at the lower dose rate were found to have slightly higher means of some cell types at days 6 and 21, these differences were not significant (Figure 2A). Similarly, qRT-PCR analysis of hematopoietic cells isolated 2 days after radiation from from non-transplanted, irradiated fish revealed no significant differences between dose-rate groups in expression levels of *cmyb, gata1*, or *mpx* (Figure 2B). Cumulatively, these results provide no evidence for differences in myelosuppression between dose-rate groups.

Figure 1.

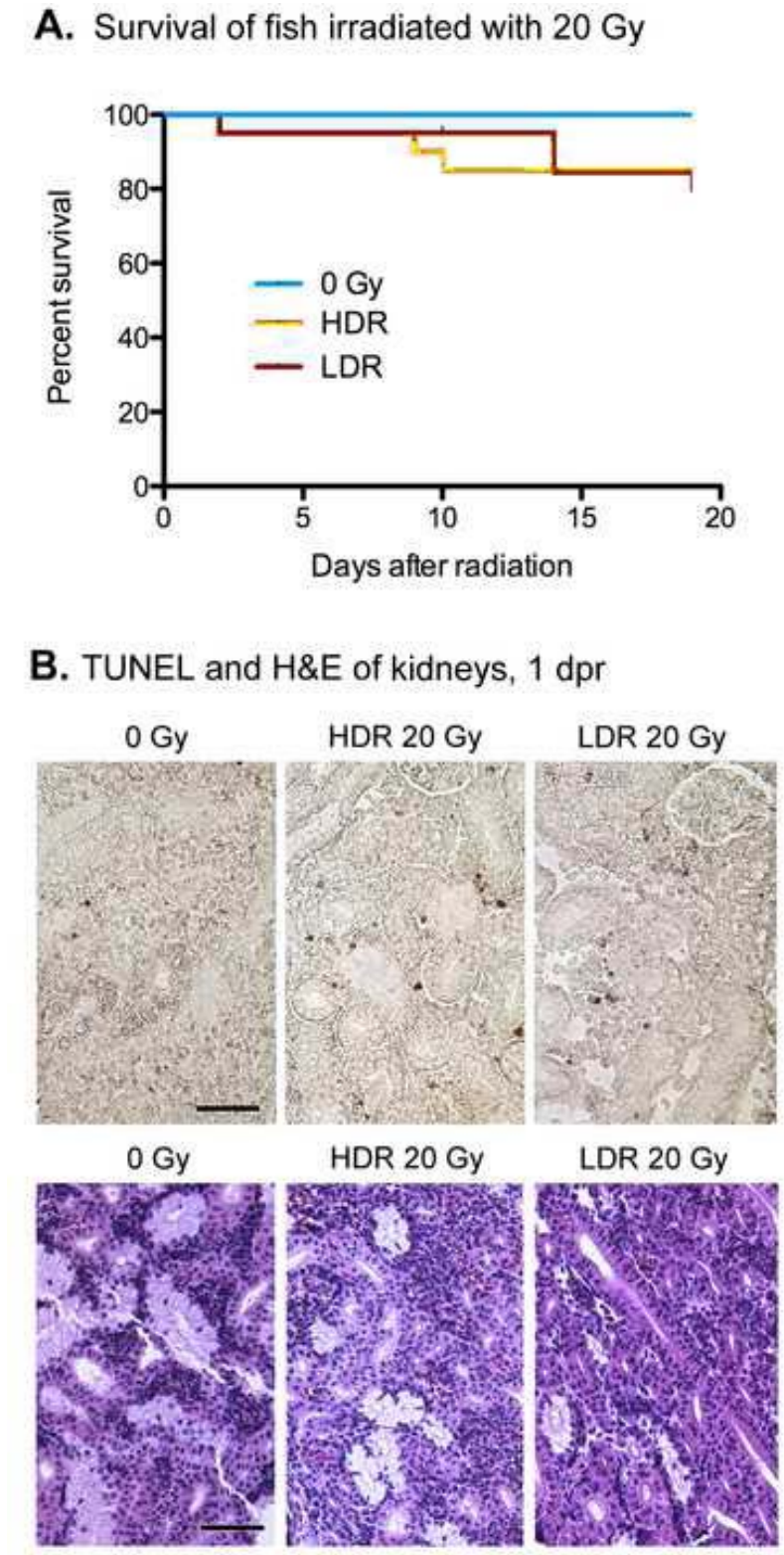
A. Survival of fish irradiated with 20 Gy
Percent survival
100
80
60
40
20
0
0 Gy
HDR
LDR
0
5
10
15
20
Days after radiation
B. TUNEL and H&E of kidneys, 1 dpr
0 Gy
HDR 20 Gy
LDR 20 Gy
0 Gy
HDR 20 Gy
LDR 20 Gy

Figure 1: Consequences of 20Gy at 25 cGy/min vs 800cGy/min in non-transplanted fish.

A, Kaplan-Meier survival curves of adult zebrafish irradiated with 20Gy at either 25cGy/min (LDR) or 800cGy/min (HDR). Pooled data from two independent trials, each composed of ten fish per group. p=.356 (Log Rank Test). B, TUNEL staining (above), and H&E staining (below) of adult zebrafish kidneys harvested one day after 20Gy radiation delivered at either 25cGy/min or 800cGy/min. C, Flow cytometry analysis of hematopoietic cell recovery in the kidney on days 2, 6, and 20-21 following radiation at either 25cGy/min or 800cGy/min, showing initial myelosuppression followed by hematopoietic recovery. Plot shows the means and SDs of pooled data from two independent biological trials, for a total of at least 7-10 fish per data point. D, qRT-PCR of hematopoietic cells 2 days post radiation. Data shows pooled results from two independent biological trials; each trial composed of 4 fish per group. No statistically significant differences were noted at any time point (Repeated Measures Anova).

Figure 2

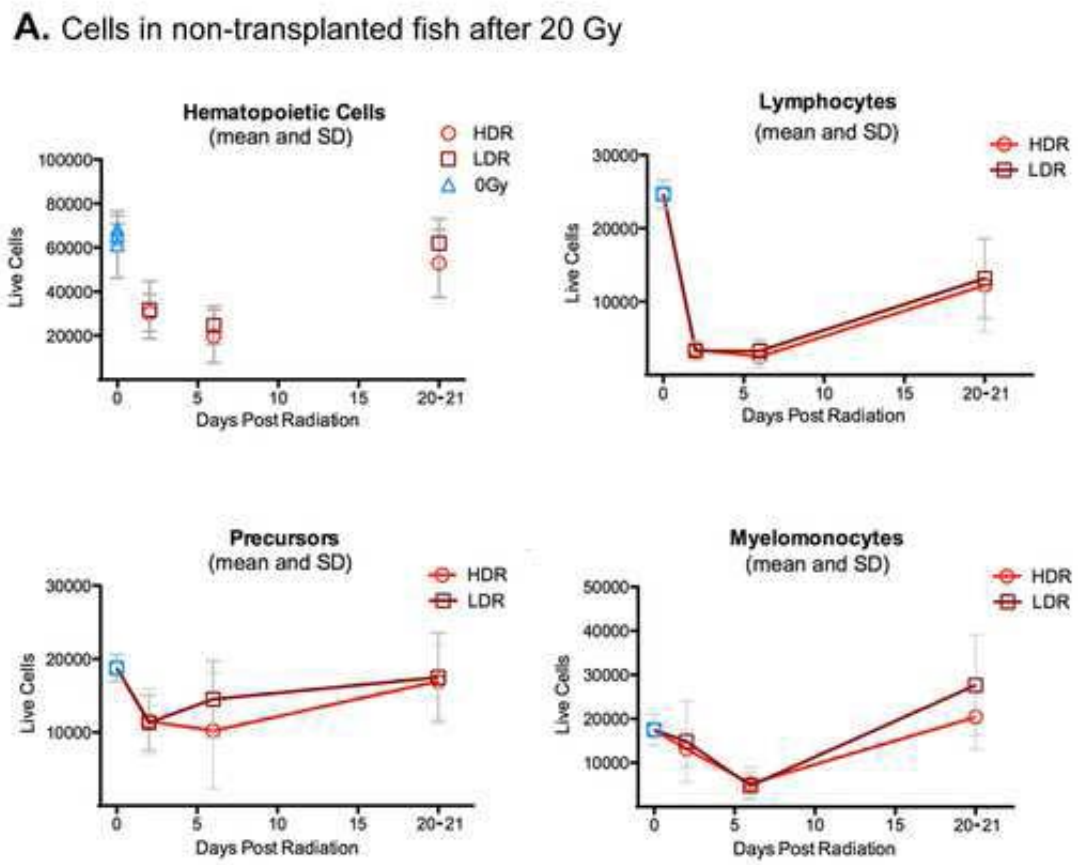
A. Cells in non-transplanted fish after 20 Gy
Hematopoietic Cells
(mean and SD)
HDR
LDR
0Gy
Live Cells
Days Post Radiation
Lymphocytes
(mean and SD)
Precursors
(mean and SD)
Myelomonocytes
(mean and SD)
B. qRT-PCR of hematopoietic cells, 2dpr
ns
0Gy
LDR
HDR
RQ
cMyb
gata1
mpx

Figure 2: Myelosuppression after 20Gy at 25 cGy/min vs 800cGy/min in non-transplanted fish.

A, Flow cytometry analysis of hematopoietic cell recovery in the kidney on days 2, 6, and 20-21 following radiation at either 25cGy/min or 800cGy/min, showing initial myelosuppression followed by hematopoietic recovery. Plot shows the means and SDs of pooled data from two independent biological trials, for a total of at least 7-10 fish per data point. B, qRT-PCR of hematopoietic cells 2 days post radiation. Data shows pooled results from two independent biological trials; each trial composed of 4 fish per group. No statistically significant differences were noted at any time point (Repeated Measures Anova).

We next assessed damage-response gene expression changes at several time points ranging from 3 hours to 2 days after radiation delivered at each of the dose rates. After radiation, samples of pooled zebrafish kidneys were processed to separate the tissues into a fraction enriched for hematopoietic cells from the kidney, and a fraction enriched for the non-hematopoietic (primarily renal tubule) cells. These fractions were then assessed separately for ddb2 and p53 gene expression changes. Ddb2 is a p53-regulated gene involved in DNA repair, which has been previously reported to undergo significant expression level changes in human radiation therapy patients, and has consequently been proposed to show potential as a biomarker of radiation response [103,104]. Although zebrafish hematopoietic cell samples showed radiation-induced changes in expression levels following radiation, no significant differences were found between the two dose rate groups (Fig 3A). Similarly, sample fractions enriched for renal tubules showed no significant differences in gene expression changes between the two

dose-rate groups (Fig 3B). Cumulatively, all of these results indicate that 20 Gy delivered at 800 cGy/min causes damage profiles that are in several aspects similar to the damage profiles caused by 20 Gy delivered at 25 cGy/min.

Effects of Dose Rates on Hematopoietic Engraftment: In order to assess the relative impacts of these radiation dose-rates on HCT in this zebrafish model, we irradiated recipients with 20 Gy at either 25 cGy/min or 800 cGy/min, transplanted each group with donor WKM from transgenic donors that constitutively expressed GFP, and used flow cytometry analysis of recipient kidneys at several time points after transplant to compare donor cell homing and engraftment between the two groups. Most strikingly, at nine days post transplant, recipients in the 800 cGy/min groups consistently contained significantly greater percentages of donor-derived cells compared to fish in the 25 cGy/min group (Figure 4A-B).

Figure 3.

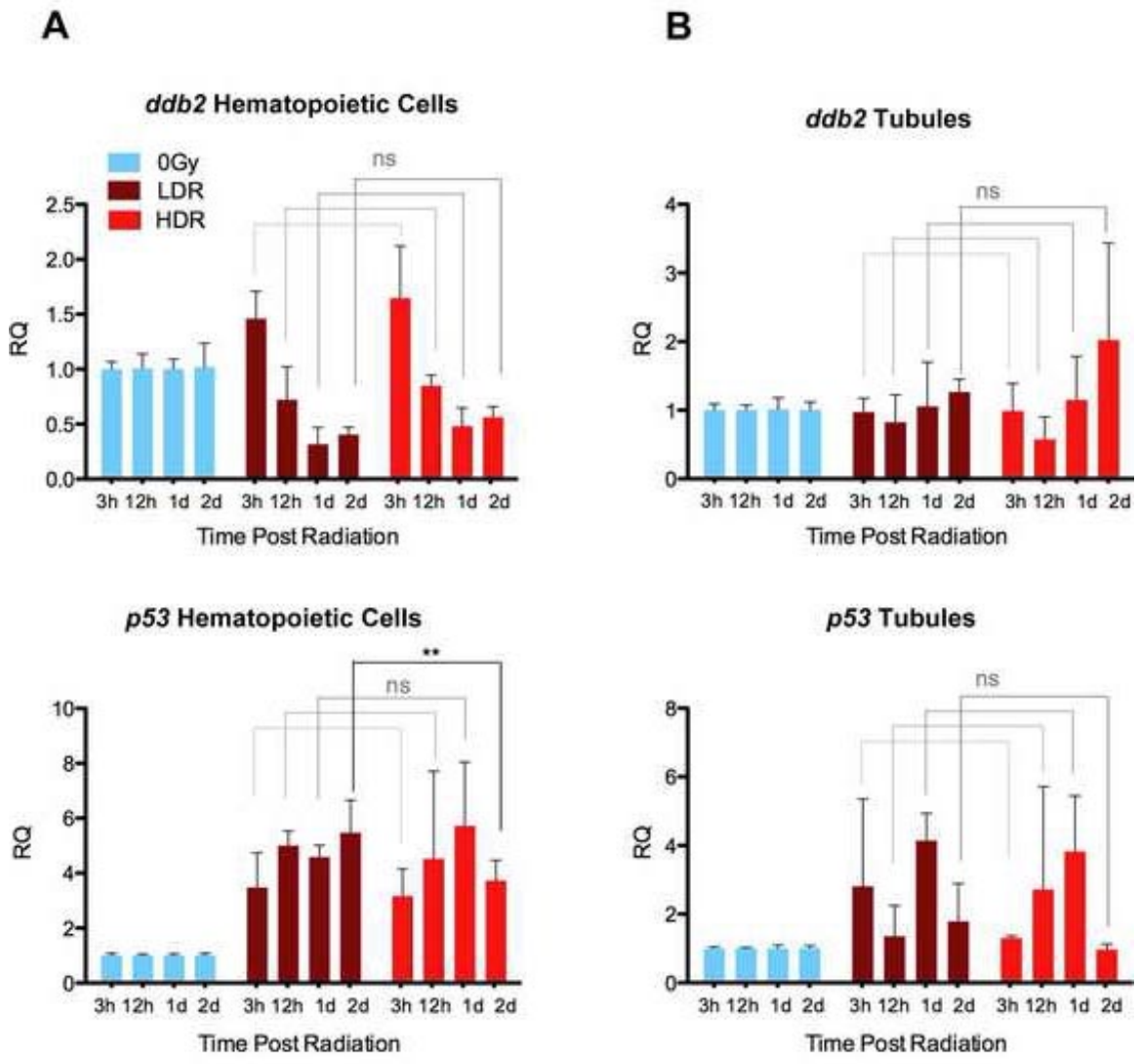
A
B
ddb2 Hematopoietic Cells
0Gy
LDR
HDR
ns
RQ
Time Post Radiation
3h 12h 1d 2d 3h 12h 1d 2d 3h 12h 1d 2d
ddb2 Tubules
p53 Hematopoietic Cells
**
p53 Tubules

Figure 3: qRT-PCR of hematopoietic and non-hematopoietic kidney after radiation.

3 hours, 12 hours, 1 day, and 2 days after 20 Gy irradiation at either a high dose rate of 800 cGy/min (HDR) or a lower dose rate of 25 cGy/min (LDR), WT zebrafish kidneys were pooled and filtered to obtain samples enriched for either hematopoietic whole kidney marrow (WKM) (A), or renal tubules (B). 0 Gy control samples were harvested concurrently at each time point and set as biological references. Each biological trial was composed of four kidneys per time point, and data summarizes pooled results from 2-3 independent biological trials per time point, per condition. Relative Quotient (RQ) differences less than two-fold were considered to be biologically non-significant. No significant differences were found between dose rate groups. (Repeated measures ANOVA and Tukey's post comparison test.)

Figure 4.

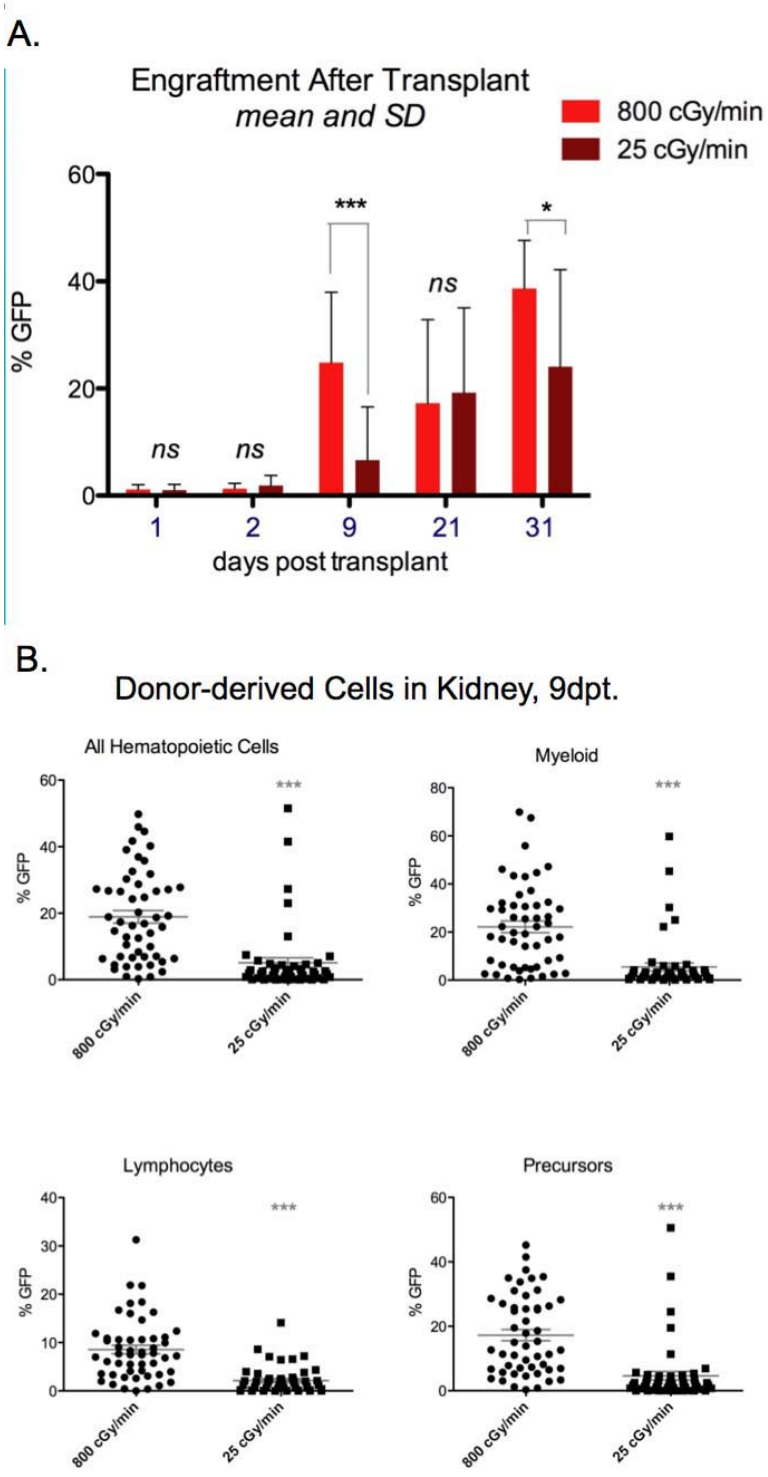
A.
Engraftment After Transplant
mean and SD
800 cGy/min
25 cGy/min
% GFP
60
40
20
0
***
*
ns
ns
ns
1
2
9
21
31
days post transplant
B.
Donor-derived Cells in Kidney, 9dpt.
All Hematopoietic Cells
Myeloid
Lymphocytes
Precursors
% GFP
800 cGy/min
25 cGy/min
***

Figure 4: Hematopoietic cell transplant after radiation

A, WT zebrafish were irradiated with 20Gy at either 800 cGy/min or 25 cGy/min, and transplanted with Bactin:GFP hematopoietic cells. At 1, 2, 9, 21, and 31 days after transplant, kidneys were harvested from recipients and isolated hematopoietic cells were analyzed by flow cytometry for percentages of GFP-positive cells. Data shows results from 10 fish per group (1 dpt), 8-10 fish per group (2 dpt), 25-26 fish per group (9dpt), 10-11 fish per group (21 dpt) and 10-13 fish per group (day 31). 9 dpt $p < 0.0001$, 31 dpt $p = 0.0301$ (unpaired t test). B, Flow cytometry analysis of hematopoietic cells isolated from transplanted fish 9 days after transplant. Each data point indicates results from one fish. Data is pooled from six biologically independent experiments; three with Bactin:GFP donor cells and three with h2afv:GFP donor cells, for cumulative totals of 51 and 48 fish in the HDR and LDR groups, respectively. $p < 0.0001$ (unpaired t test)

Anatomical Characteristics of Engraftment 9 Days Post Transplant:

Because dose-rate was found to impact hematopoietic reconstitution as early as 9 dpt, fluorescence microscopy was used to assess localization of donor-derived cells at that time point. Whole body fluorescence detection of the living fish showed donor-derived cells distributed throughout the body in both dose rate groups at that time point. Recipients irradiated at 800 cGy/min showed a non-significant trend toward higher levels of donor-derived fluorescence signal (p=.06) (Figure 5A). 9 days after WT fish were transplanted with GFP-labeled cells, *ex vivo* preparations of their kidneys periodically reveal highly localized concentrations of donor-derived cells (Figure 5B). Because previous studies have suggested renal tubule cells may help form the hematopoietic stem and progenitor cell niche in this organism [66,97], and might therefore be expected to support localized hematopoietic proliferation, we next assessed kidney preparations of Tg(*sdf-1a:DsRed*) transplant recipients. Tg(*sdf-1a:DsRed*) fish allow fluorescence detection of subsets of renal tubules that express high levels of *sdf-1*. However, despite the presence of donor-derived cells adjacent to *sdf-1a:DsRed* structures in both groups, anatomical expression patterns of *sdf-1a* expression in the kidney did not appear to uniquely correlate with the specific concentrations of donor-derived cells that appeared primarily in the HDR group (Fig 5C).

Figure 5.

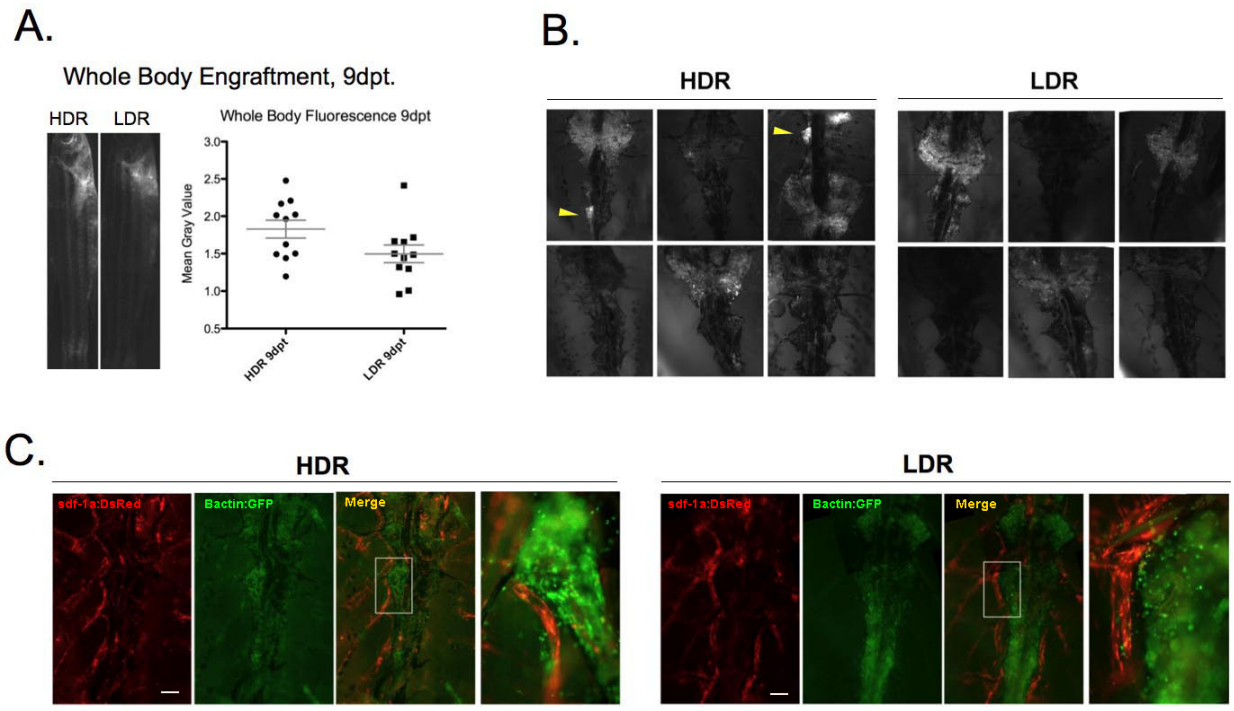

Figure 5. Anatomical characteristics of hematopoietic reconstitution 9dpt

A) Fish were irradiated with 20 Gy at either a high dose rate of 800 cGy/min (HDR) or lower dose rate of 25 cGy/min (LDR), and transplanted with Bactin:GFP WKM cells. 9 days after transplant (dpt), live fish were photographed to record whole-body GFP signal. Mean gray values were obtained from photo composites of each fish. Representative photographs show the approximate mean gray value of each group. Data shows results pooled from two independent biological experiments, for a total of 11 fish per group. B) Fresh kidneys were photographed to detect GFP signal 9 dpt, six fish per group. Sites with exceptionally high concentrations of donor-derived cells are indicated with yellow arrowheads. C) Tg(sdf-1a:DsRed) recipients were transplanted with Bactin:GFP WKM cells. 9 dpt, kidneys from each group were photographed to document sdf-1a:DsRed and Bactin:GFP expression. Region of enlargement was chosen based on anatomical similarity to indicated regions in panel B. No HDR-specific expression patterns of *sdf-1a* were noted. scale, 200 uM.

The sdf-1a/cxcr4b Axis is Not Required for Improved Engraftment 9 dpt in Recipients Conditioned at 800 cGy/min: In light of the fact that previous studies have reported radiation-induced changes in *sdf-1* expression levels [97], and reports have also suggested roles for SDF-1 in hematopoietic cell survival and proliferation [105], we next sought to assess the functional relevance of SDF-1 to the improved engraftment 9 dpt in high dose-rate conditioned fish. To this end, WT zebrafish were preconditioned as before and transplanted with Tg(*Bactin:EGFP*) cells that were also either heterozygous or homozygous for the loss of function in the cxcr4b receptor for sdf-1a *(odysseus* mutation). 9 days after transplant, recipient kidneys were harvested and assessed by flow cytometry. Both heterozygous and homozygous *odysseus* hematopoietic cells showed greater percentages of donor-derived cells 9 days after transplant in the higher dose-rate groups (Figure 6A). Additionally, qRT-PCR assays detected no significant differences in expression levels of *sdf-1a* between irradiated WT fish in the two dose-rate groups. As donor cells insensitive to the *sdf-1a/cxcr4b* axis were capable of showing the dose-rate effect after transplant, and comparison of the two dose-rates in non-transplanted fish revealed no significant differences in *sdf-1*a levels induced by the preconditioning rates, we conclude that the *sdf-1a/cxcr4b* axis is likely not required for the observed impact of radiation dose-rate on engraftment.

Figure 6.

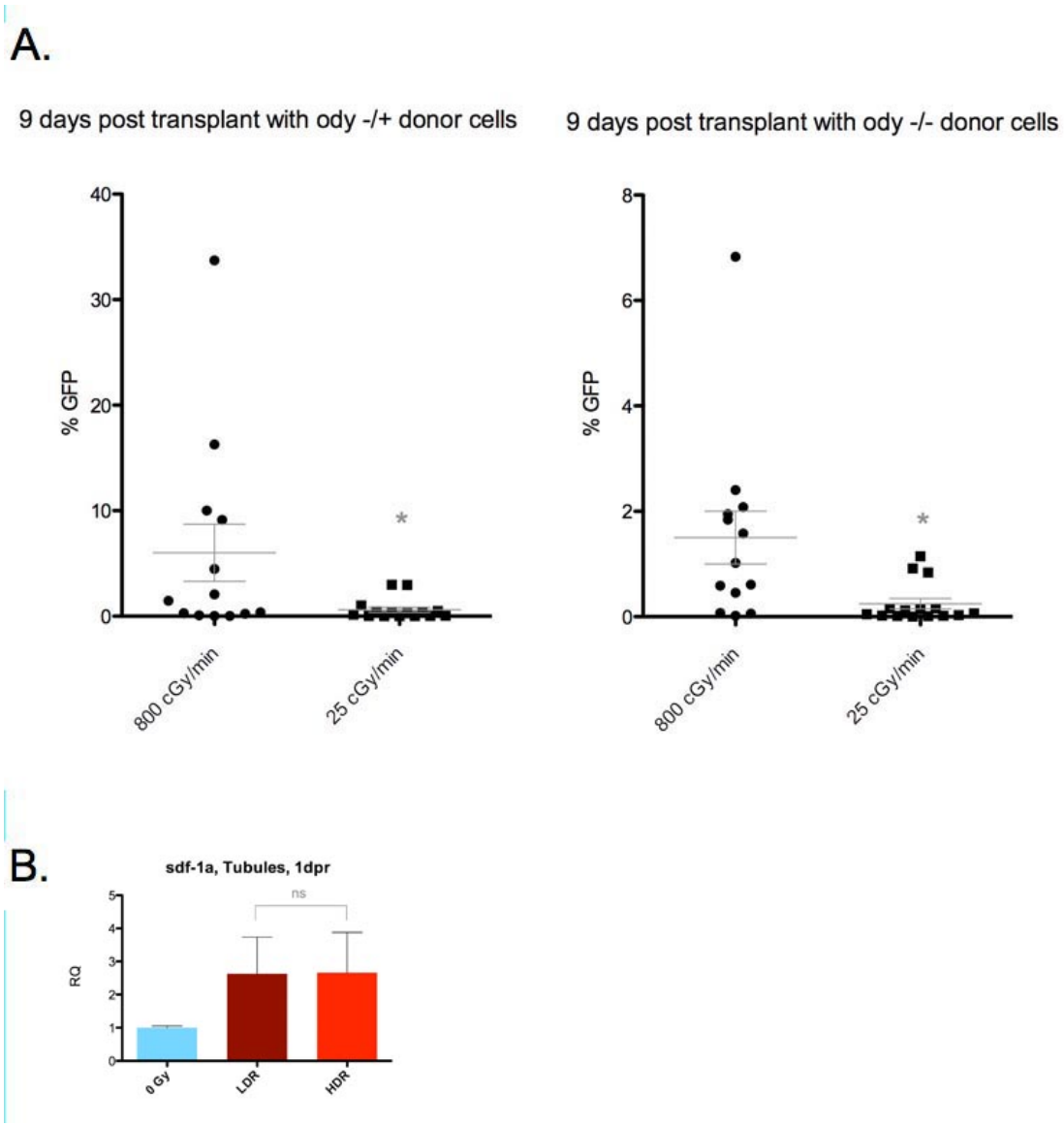

Figure 6: Dose-Rate effect does not require cxcr4b in transplanted cells.

A) WT zebrafish were irradiated with 20 Gy at either dose rate and transplanted with Tg(Bactin:GFP) WKM that was either heterozygous or homozygous for the *odysseus* (*cxcr4b*) mutation. 9 dpt, kidneys were analyzed by flow cytometry. Pooled results from two biologically independent trials, n=13-15 fish per group. Heterozygous: p= 0.0420, Homozygous: p= 0.0141, (unpaired t-test). B) 1 day after radiation, samples enriched for renal tubules were collected from WT fish and analyzed by qRT-PCR for sdf-1a. No biologically significant differences were seen

between dose-rate groups. Pooled results shown from two biological experiments, each experiment n=4 fish per group.

Discussion

This study compared outcomes in adult zebrafish conditioned with a sublethal radiation dose delivered at either 25 cGy/min or 800 cGy/min. While striking differences between the dose-rate groups in parameters of cell death, myelosuppression, gene expression indicators of DNA damage, and hematopoietic cell homing were not detected at early time points after radiation, recipient fish did show a significant dose-rate dependent effect in early engraftment 9 and 31 days after HCT. Our findings of biologically comparable outcomes in the two dose rate groups at time points 1-2 days after radiation are consistent with the findings of a previous study of radiation dose-rate and HCT in mice, which found dose-rates ranging from 10 cGy/min to 585 cGy/min produced no substantial differences between groups in homing of lineage-depleted cells 2 dpt, but did show a small increase in donor-derived cells in bone marrow 5 dpt in the highest dose rate group [2]. This study as well as our own suggest that salient effects specific to radiation dose-rate in transplanted organisms may begin to emerge approximately a week after transplant. The mechanisms responsible for these effects are somewhat unclear. Although many effects of radiation have been traditionally attributed to immediate cell damage directly caused by the radiation, secondary bystander effects can have substantial impacts as well, but may manifest at a variety of later time periods following radiation delivery [106].

In HCT, conditioning radiation initially causes cell death and myelosuppression, also elicits responses from the recipient tissues that can alter donor-derived cell migration and engraftment [10 9 107], and thirdly can cause both acute and long-term off-target toxicities and pathologies [12,108]. Our investigation revealed no significant differences in myelosuppression or early toxicity between the dose-rate groups. This finding is not unlike those of previous studies of lower ranges of radiation dose-rates using gamma and proton irradiation, which have collectively reported dose-rate effects on indicators of myelosuppression to be either non-significant, or moderately greater in some hematopoietic cell subsets in HDR groups [89,109-111]. However, the likelihood that higher dose-rates will more effectively suppress important functional subset of recipient immune cells merits continued recognition in light of previous work linking radiation dose-rate to more significantly improved engraftment in allogeneic, rather than syngenic, transplants, in comparisons of 2cGy/min to 40cGy/min [93]. Future inquiry using the zebrafish model system will be aided by the development of more refined methods for the identification of functional subsets of hematopoietic populations in the fish, which may permit the discovery of dose-rate-specific myelosuppressive differences that are undetectable with the methods used in this study.

Apart from toxicity and myelosuppression, it has yet to be determined whether very high dose-rates can induce changes in the microenvironment of the hematopoietic tissues by modulating factors that direct donor cell migration,

behavior, and proliferation, thereby influencing rate of engraftment. Sdf-1 has been previously shown to elicit homing in this model system [97]. However, we find it does not show differences in up-regulation between the high and low dose rate groups, nor do we observe differences in homing between the dose rate groups. Combined with the finding that the dose-rate effect is preserved in transplants of *odysseus* cells insensitive to Sdf-1a, it is reasonable to conclude that donor cell responses to the sdf-1a/cxcr4 axis are not required for the observed dose-rate effect. It bears mentioning that the *odysseus* mutant shows uncharacterized yet readily apparent hematopoietic abnormalities compared to WT fish (data not shown), raising the possibility that the consequences of Sdf-1 insensitivity in *ody* cells include aspects of hematopoietic differentiation, proliferation, or survival. Although this does not necessarily mitigate the finding that the *sdf-1a/cxcr4b* axis is not required for the radiation dose-rate effect, it does suggests an avenue of investigation by which additional donor-specific mechanisms could be ruled out.

Zebrafish do show some significant differences from mammals in response to radiation, due at least in part to the radioprotective consequences of being cold-blooded, as has been discussed previously [96]. However, as previous studies report similarities between zebrafish and humans in several aspects of hematopoietic biology that are highly relevant to HCT outcomes [97,112] it is reasonable to expect that the zebrafish transplant model will continue to be informative to future dose-rate investigations.

Chapter 4:

Conclusion and Potential Applications of Findings

Cumulatively, this work validates the adult zebrafish model for biological investigations of the chemokine Sdf-1 and the impacts of radiation dose-rate effects as they pertain to HCT. In light of the particular methodological strengths and biological attributes of the zebrafish model, these findings lay the groundwork for new avenues of inquiry.

1. Applications to the study of endogenous HSC homing and moblilization

Mobilization of Hematopoietic Stem and Progenitor Cells (HSPC) from the bone marrow to the circulation occurs in mammals on a circadian cycle by a sdf-1/cxcr4-dependent pathway [7]. It is currently unknown if this cyclic mobilization is a phenomenon that is unique to mammals, and the purpose of endogenous cyclic HSC mobilization is also currently unknown. It has been speculated that the biological purpose for endogenous cyclic HSC mobilization is to facilitate effective bone remodeling [113], which, if true, would suggest it should be a phenomenon specific to organisms with bone marrow. Since zebrafish do not have bone marrow (their hematopoiesis occurs in the kidney), our understanding of the functions served by this cyclic mobilization would be advanced by determining whether zebrafish show endogenous sdf-1-drived cycles of HSPC moblilization. Our work has recently demonstrated that multiple aspects of Sdf-1 driven hematopoietic cell migration are conserved in the zebrafish, which makes the investigation of endogenous Sdf-1 driven HSPC migrations in this model quite possible.

In mammals, expression of adrenergic receptors by bone marrow hematopoietic support cells has been suggested to provide a mechanism through which the central nervous system modulates hematopoietic cell behavior. Release of noradrenaline at sites of sympathetic innervation in the bone marrow activates adrenergic receptors in the HSC niche, which respond in a cascade that ultimately downregulates *sdf-1*. Acutely lowered sdf-1 in the bone marrow induces the mobilization of HSC from the bone marrow niche into the circulation. In this way, the sympathetic nervous system is thought to direct circadian cycles of endogenous hematopoietic mobilization and homing [7,114].

To determine whether adult zebrafish kidneys show anatomical prerequisites for sympathetic modulation of HSC mobilization from the kidney, whole mount staining for tyrosine hydroxylase (TH) was performed on kidneys to reveal sympathetic innervation of this organ (Figure 1). Staining revealed TH-positive ganglia throughout the adult kidney, as well as adjacent localizations of TH-positive processes along sdf-1a:DsRed-positive renal tubules (Figure 1B,C). Since beta-adrenergic receptor activation has been identified in mammals as the means by which SDF-1+ stromal cells in the bone marrow detect sympathetic cues directing the reduction of sdf-1 expression levels, we performed RT-PCR to determine whether adrenergic receptor expression was impacted by preconditioning radiation, and found downregulation in tubules 1 day after 30Gy.

Figure 1.

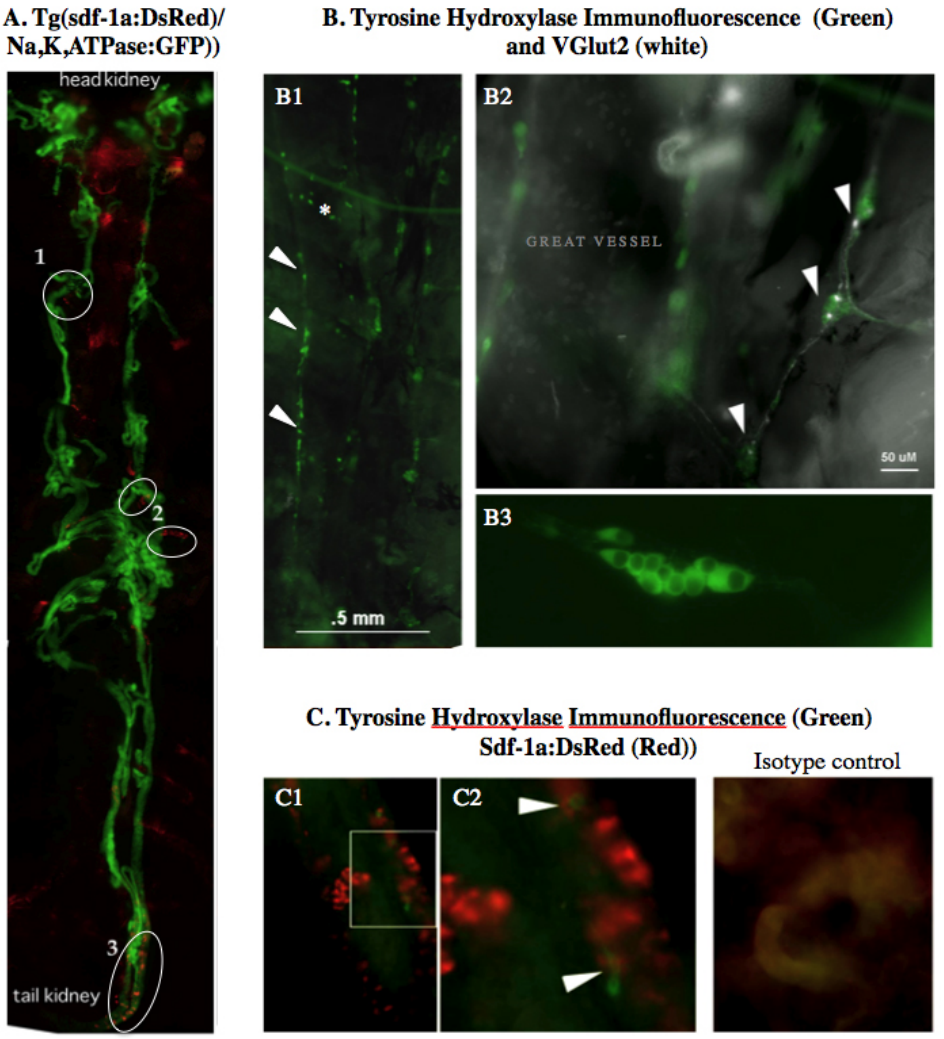
A. Tg(sdf-1a:DsRed)/
Na,K,ATPase:GFP))
head kidney
1
2
3
tail kidney
B. Tyrosine Hydroxylase Immunofluorescence (Green)
and VGlut2 (white)
B1
.5 mm
B2
GREAT VESSEL
50 uM
B3
C. Tyrosine Hydroxylase Immunofluorescence (Green)
Sdf-1a:DsRed (Red))
Isotype control
C1
C2

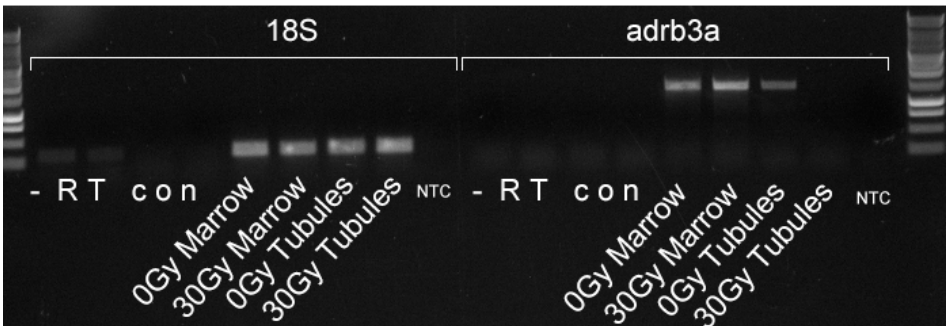
D. Impact of Radiation on Beta-Adrenergic Receptor Expression in Kidney
18S
adrb3a
- RT con
0Gy Marrow
30Gy Marrow
0Gy Tubules
30Gy Tubules
NTC
- RT con
0Gy Marrow
30Gy Marrow
0Gy Tubules
30Gy Tubules
NTC

Figure 1. Potential Sources of Sympathetic Innervation Adjacent to *sdf-1a:DsRed* Niche Cells in the Fish Kidney

A. Fresh intact kidney of a double transgenic reveals sdf-1a:DsRed niche cells composing either proximal tubules (1,2) or distal tubules (3). **B1**. Whole-mount immunofluorescence of adult zebrafish kidney reveals Tyrosine Hydroxylase positivity flanking the great vessels (arrows) and in putative chromaffin cells (*), as well as strong staining in the head kidney (not shown). **B2** Detail of B1, indicating Tyrosine-Hydroxylase positive ganglia (green) containing Vglut2-positive cells (glutamatergic neurons). **B3.** Enlargement of a typical ganglion demonstrates characteristic morphology similar to that shown of sympathetic ganglia previously described. **C1.** Double Whole Mount Immunofluorescence for TH (Green) and sdf-1a:DsRed (Red) reveals adjacent localization of the two cell types. **C2.** Enlarged detail demonstrates TH-positive cells located on sdf-1a:DsRed tubules (arrows). **D,** Preliminary RT-PCR for beta-adrenergic receptor (adrb3a) expression levels in zebrafish kidney samples suggest down-regulation of expression after 30Gy radiation in renal tubules. Similar results were obtained for adrb3b (data not shown). Samples were collected at 1 day post radiation, which coincided with radiation-induced increases in *sdf-1* levels. One biological trial, composed of pooled material from approximately 10 adult WT fish. NTC = No Template Control, -RTcon = reverse transcriptase-negative control.

Although preliminary, these findings raise the possibility that preconditioning radiation may alter sdf-1 expression levels at least in part through its impacts on this endogenous neuroreticular system. As an endogenous system to enforce hematopoietic homeostasis likely involved a variety of at least partially redundant mechanisms, it is possible that this system may be pertinent to other inquires, such as the mechanisms by which radiation dose-rate impacts donor-derived hematopoietic reconstitution. In the future, a clear understanding of the endogenous mechanisms enforcing HSC mobilization and homing may allow

more refined evaluation of current radiation preconditioning strategies that either promote or counteract endogenous pathways for HSC mobilization and homing. This should assist the exploitation of endogenous pathways to advance therapeutic goals.

2. Applications to the study of extramedullary HSC migration after HCT

A second potentially valuable avenue of investigation which is now possible due to our findings, and for which the adult zebrafish model is uniquely well-suited, is the interrogation of preconditioning radiation's impact on extramedullary HSC migration after transplant. Currently, exceptionally high dose-rates of radiation, such as the high rate investigated in this dissertation, are delivered not to the entire body, but to precisely targeted locations such as the bone marrow only. This is referred to as Total Marrow Irradiation (TMI), and compares to the more common current standard of radiation preconditioning by Total Body Irradiation (TBI), in which radiation is delivered essentially to the entire body. It has been well-documented that after TBI and transplant, transplanted cells have been found in locations throughout the body. The migration of HSCs to extramedullary regions may lower the homing efficiency of HCT.

Previous suggestions that extramedullary SDF-1 expression attracts HSPCs to sites of injury[115], coincide with our own findings in zebrafish that *sdf-1* levels increase in skin after radiation, and attract migrating donor-derived cells.

With currently existing technology it would be possible to deliver high dose-rate radiation to only the kidney region of the zebrafish, while sparing head, abdomen, and tail, thereby more closely approximating the spatial fidelity of TMI deliveries. This, combined with our completed basic assessment of high dose-rate radiation conditioning responses in fish, and our completed assessments of Sdf-1-driven hematopoietic migration in fish, collectively lay the necessary groundwork for studying the unique impacts of high dose-rate TMI on extramedullary migration following HCT. This interrogation would allow the continuing refinements of radiation conditioning technologies to be paralleled by advances in our understanding of their biological effects as they pertain to HCT.

3. Applications to the study of perivascular cells

Thirdly, characterization of Tg(sdf-1a:DsRed) led us to serendipitous discoveries of many previously uncharacterized cell types in the adult zebrafish which express high levels of this chemokine. These include sdf-1a+ perivascular cells throughout the body of the organism. Although these unique cells can be moderately difficult to find in histological sections due to their intermittent distribution, they are fairly easily observed through the whole-body epifluorescence microscopy routinely used in living adult zebrafish. These cells may ultimately prove informative to future investigations of cell migration, vascular remodeling, and the chemoattractant mechanisms that enforce anatomical assembly of neurovascular structures.

Pericytes have been reported to participate in several processes of pertinence to human health and disease. These include regulation of microvascular permeability, regulation of perivascular extracellular matrix (ECM) composition, regulation of vessel diameter and blood flow, and perivascular phagocytosis [116]. In *Tg(sdf-1a:DsRed)*, *sdf-1a:DsRed* perivascular cells are located in skin, fin, eyes, kidney, brain, and quite prominently along what are likely thoracic neurovascular bundles. Many of these sites are located superficially in the organism, and are therefore readily accessible to *in-vivo* video-microscopy in the living organism; allowing real-time observation of pericyte behavior, vessel constriction, remodeling, and blood flow. Because the pericytes visible in the transgenic reporter system specifically express high levels of Sdf-1, which chemoattracts a variety of different cell types, the potential functions of these pericytes might be anticipated to involve their influence on neighboring cells. As described below, pilot experiments have suggested several possibilities for the roles these cells play in maintaining organism homeostasis.

First, there is preliminary evidence that at least a subset of putative pericytes in *Tg(sdf-1a:DsRed)* may respond to adjacent cell injury. Previous reports describe a system for exogenous application of ATP to tissue in order to mimic endogenous signals of tissue damage [117]. In deeply anesthetized fish, ATP in solution applied to the skin of the zebrafish coincides with video recording of *sdf-1a:DsRed* pericyte initiation of cell motility and movement along the long axis of the vessel. If this result were to become significant under future sustained

investigation, it would suggest that extracellular cell damage cues may trigger rapid movement of at least a subset of these cells along the vessels. Secondly, similar video photomicrography methods have captured putative microvascular remodeling events in the skin of *Tg(sdf-1a:DsRed)/Tg(fli:GFP)* transgenic fish, in which rapid extensions of a *fli:GFP* endothelial protrusion orthogonal to the long axis of the vessel is followed in short order by movement of a *sdf-1a:DsRed* pericyte to engulf and remove the vascular extension. Collectively, these preliminary results highlight the feasibility of using this system to interrogate real-time perivascular responses to tissue injury and vascular remodeling events.

Bibliography

1. P. Jan Hendrikx JWMV. Homing of fluorescently labeled murine hematopoietic stem cells. *Experimental Hematology*. 1996;24:129-140.
2. Collis SJ, Neutzel S, Thompson TL, et al. Hematopoietic progenitor stem cell homing in mice lethally irradiated with ionizing radiation at differing dose rates. *Radiat Res*. 2004;162(1):48-55.
3. Askenasy N, Stein J, Yaniv I, Farkas DL. The topologic and chronologic patterns of hematopoietic cell seeding in host femoral bone marrow after transplantation. *Biol Blood Marrow Transplant*. 2003;9(8):496-504.
4. Lapidot T, Dar A, Kollet O. How do stem cells find their way home? *Blood*. 2005;106(6):1901.
5. Katayama Y, Hidalgo A, Peired A, Frenette PS. Integrin alpha4beta7 and its counterreceptor MAdCAM-1 contribute to hematopoietic progenitor recruitment into bone marrow following transplantation. *Blood*. 2004;104(7):2020-2026.
6. Peled A, Kollet O, Ponomaryov T, et al. The chemokine SDF-1 activates the integrins LFA-1, VLA-4, and VLA-5 on immature human CD34+ cells: role in transendothelial/stromal migration and engraftment of NOD/SCID mice. *Blood*. 2000;95(11):3289.

7. Méndez-Ferrer S, Lucas D, Battista M, Frenette P. Haematopoietic stem cell release is regulated by circadian oscillations. *Nature*. 2008;452(7186):442-447.
8. FERREBEE JW, THOMAS ED. Radiation injury and marrow replacement: factors affecting survival of the host and the homograft. *Ann Intern Med*. 1958;49(5):987-1003.
9. Gaugler MH, Squiban C, Mouthon MA, Gourmelon P, van der Meeren A. Irradiation enhances the support of haemopoietic cell transmigration, proliferation and differentiation by endothelial cells. *Br J Haematol*. 2001;113(4):940-950.
10. Bastianutto C, Mian A, Symes J, et al. Local Radiotherapy Induces Homing of Hematopoietic Stem Cells to the Irradiated Bone Marrow. *Cancer Res*. 2007;67(21):10112-10116.
11. Fortin A, Benabdallah B, Palacio L, et al. A soluble granulocyte colony stimulating factor decoy receptor as a novel tool to increase hematopoietic cell homing and reconstitution in mice. *Stem Cells Dev*. 2013;22(6):975-984.
12. Bentzen SM. Preventing or reducing late side effects of radiation therapy: radiobiology meets molecular pathology. *Nat Rev Cancer*. 2006;6(9):702-713.
13. Rosse Wa. Distribution and Identity of the Earliest Proliferating Progeny of Colony-Forming Cells in Regenerating Murine Spleen and Bone Marrow. *THE AMERICAN JOURNAL OF ANATOMY*. 1982;**163**:**131-140**.
14. Till JE, McCulloch EA. A Direct Measurement of the Radiation Sensitivity of Normal Mouse Bone Marrow Cells. *Radiation Research*. 1961;14(2):213-222.
15. Cao Y, Wagers A, Beilhack A, et al. Shifting foci of hematopoiesis during reconstitution from single stem cells. *Proceedings of the National Academy of Sciences*. 2004;101(1):221-226.
16. Akpek G, Pasquini MC, Logan B, et al. Effects of spleen status on early outcomes after hematopoietic cell transplantation. *Bone Marrow Transplant*. 2012.
17. Tricot G, Jagannath S, Vesole D, et al. Peripheral blood stem cell transplants for multiple myeloma: identification of favorable variables for rapid engraftment in 225 patients. *Blood*. 1995;85(2):588-596.
18. Dubovsky J, Daxberger H, Fritsch G, et al. Kinetics of chimerism during the early post-transplant period in pediatric patients with malignant and non-malignant hematologic disorders: implications for timely detection of engraftment, graft failure and rejection. *Leukemia*. 1999;13(12):2059, 2060-2059.
19. Baron F, Little MT, Storb R. Kinetics of engraftment following allogeneic hematopoietic cell transplantation with reduced-intensity or nonmyeloablative conditioning. *Blood Rev*. 2005;19(3):153-164.
20. Manning DD, Reed ND, Shaffer CF. Maintenance of skin xenografts of widely divergent phylogenetic origin of congenitally athymic (nude) mice. *J Exp Med*. 1973;138(2):488-494.
21. Baron F, Baker JE, Storb R, et al. Kinetics of engraftment in patients with hematologic malignancies given allogeneic hematopoietic cell transplantation after nonmyeloablative conditioning. *Blood*. 2004;104(8):2254-2262.
22. Kelly RM, Highfill SL, Panoskaltsis-Mortari A, et al. Keratinocyte growth factor and androgen blockade work in concert to protect against conditioning regimen-induced

thymic epithelial damage and enhance T-cell reconstitution after murine bone marrow transplantation. *Blood*. 2008;111(12):5734-5744.
23. Kelly RM, Goren EM, Taylor PA, et al. Short-term inhibition of p53 combined with keratinocyte growth factor improves thymic epithelial cell recovery and enhances T-cell reconstitution after murine bone marrow transplantation. *Blood*. 2010;115(5):1088-1097.
24. Li HW, Sykes M. Emerging concepts in haematopoietic cell transplantation. *Nat Rev Immunol*. 2012;12(6):403-416.
25. Zhang Y, Adachi Y, Suzuki Y, et al. Synergistic effects of granulocyte-colony stimulating factor and macrophage-colony stimulating factor on recovery of donor hematopoietic cells in allogeneic bone marrow transplantation. *Oncol Rep*. 2006;16(2):367-371.
26. Nagasawa T. A chemokine, SDF-1/PBSF, and its receptor, CXC chemokine receptor 4, as mediators of hematopoiesis. *Int J Hematol*. 2000;72(4):408-411.
27. Singh VK, Fatanmi OO, Singh PK, Whitnall MH. Role of radiation-induced granulocyte colony-stimulating factor in recovery from whole body gamma-irradiation. *Cytokine*. 2012;58(3):406-414.
28. Tashiro K, Tada H, Heilker R, Shirozu M, Nakano T, Honjo T. Signal sequence trap: a cloning strategy for secreted proteins and type I membrane proteins. *Science*. 1993;261(5121):600-603.
29. Nagasawa T, Kikutani H, Kishimoto T. Molecular cloning and structure of a pre-B-cell growth-stimulating factor. *Proc Natl Acad Sci U S A*. 1994;91(6):2305-2309.
30. Egawa T, Kawabata K, Kawamoto H, et al. The earliest stages of B cell development require a chemokine stromal cell-derived factor/pre-B cell growth-stimulating factor. *Immunity*. 2001;15(2):323-334.
31. Tachibana K, Hirota S, Iizasa H, et al. The chemokine receptor CXCR4 is essential for vascularization of the gastrointestinal tract. *Nature*. 1998;393(6685):591-594.
32. Bleul C, Fuhlbrigge R, Casasnovas J, Aiuti A, Springer T. A highly efficacious lymphocyte chemoattractant, stromal cell-derived factor 1 (SDF-1). *Journal of Experimental Medicine*. 1996;184(3):1101.
33. Netelenbos T, Zuijderduijn S, Van Den Born J, et al. Proteoglycans guide SDF-1-induced migration of hematopoietic progenitor cells. *J Leukoc Biol*. 2002;72(2):353-362.
34. Pesek G, Cottler-Fox M. Hematopoietic stem cell mobilization: a clinical protocol. *Methods Mol Biol*. 2012;904:69-77.
35. Kang Y, Chen BJ, Deoliveira D, Mito J, Chao NJ. Selective enhancement of donor hematopoietic cell engraftment by the CXCR4 antagonist AMD3100 in a mouse transplantation model. *PLoS One*. 2010;5(6):e11316.
36. Carradice D, Lieschke GJ. Zebrafish in hematology: sushi or science? *Blood*. 2008;111(7):3331-3342.
37. Ridges S, Heaton WL, Joshi D, et al. Zebrafish screen identifies novel compound with selective toxicity against leukemia. *Blood*. 2012;119(24):5621-5631.
38. North TE, Goessling W, Walkley CR, et al. Prostaglandin E2 regulates vertebrate haematopoietic stem cell homeostasis. *Nature*. 2007;447(7147):1007-1011.

39. Durand EM, Zon LI. Newly emerging roles for prostaglandin E2 regulation of hematopoiesis and hematopoietic stem cell engraftment. *Curr Opin Hematol*. 2010;17(4):308-312.
40. Hwang M, Yong C, Moretti L, Lu B. Zebrafish as a model system to screen radiation modifiers. *Curr Genomics*. 2007;8(6):360-369.
41. McAleer MF, Davidson C, Davidson WR, et al. Novel use of zebrafish as a vertebrate model to screen radiation protectors and sensitizers. *Int J Radiat Oncol Biol Phys*. 2005;61(1):10-13.
42. Langenau D, Ferrando A, Traver D, et al. In vivo tracking of T cell development, ablation, and engraftment in transgenic zebrafish. *Proceedings of the National Academy of Sciences of the United States of America*. 2004;101(19):7369.
43. Bertrand JY, Kim AD, Teng S, Traver D. CD41+ cmyb+ precursors colonize the zebrafish pronephros by a novel migration route to initiate adult hematopoiesis. *Development*. 2008;135(10):1853-1862.
44. Stachura DL, Svoboda O, Lau RP, et al. Clonal analysis of hematopoietic progenitor cells in the zebrafish. *Blood*. 2011;118(5):1274-1282.
45. Stachura DL, Reyes JR, Bartunek P, Paw BH, Zon LI, Traver D. Zebrafish kidney stromal cell lines support multilineage hematopoiesis. *Blood*. 2009;114(2):279-289.
46. Pedroso GL, Hammes TO, Escobar TD, Fracasso LB, Forgiarini LF, da Silveira TR. Blood collection for biochemical analysis in adult zebrafish. *J Vis Exp*. 2012(63):e3865.
47. Yaniv K, Isogai S, Castranova D, Dye L, Hitomi J, Weinstein BM. Live imaging of lymphatic development in the zebrafish. *Nat Med*. 2006;12(6):711-716.
48. van der Putte SC. The early development of the lymphatic system in mouse embryos. *Acta Morphol Neerl Scand*. 1975;13(4):245-286.
49. Postlethwait JH, Yan YL, Gates MA, et al. Vertebrate genome evolution and the zebrafish gene map. *Nat Genet*. 1998;18(4):345-349.
50. Knaut H, Werz C, Geisler R, Nüsslein-Volhard C, Consortium TS. A zebrafish homologue of the chemokine receptor Cxcr4 is a germ-cell guidance receptor. *Nature*. 2003;421(6920):279-282.
51. Traver D, Winzeler A, Stern H, et al. Effects of lethal irradiation in zebrafish and rescue by hematopoietic cell transplantation. *Blood*. 2004;104(5):1298.
52. Zon LI, Peterson RT. In vivo drug discovery in the zebrafish. *Nature Reviews Drug Discovery*. 2005;4(1):35-44.
53. Sugiyama T, Kohara H, Noda M, Nagasawa T. Maintenance of the hematopoietic stem cell pool by CXCL12-CXCR4 chemokine signaling in bone marrow stromal cell niches. *Immunity*. 2006;25(6):977-988.
54. Tashiro K, Tada H, Heilker R, Shirozu M, Nakano T, Honjo T. Signal sequence trap: a cloning strategy for secreted proteins and type I membrane proteins. *Science*. 1993;261(5121):600.
55. Pablos J, Amara A, Bouloc A, et al. Stromal-cell derived factor is expressed by dendritic cells and endothelium in human skin. Vol. 155: ASIP; 1999:1577-1586.

56. Godot V, Arock M, Garcia G, et al. H4 histamine receptor mediates optimal migration of mast cell precursors to CXCL12. *The Journal of Allergy and Clinical Immunology*. 2007;120(4):827-834.
57. Grunewald M, Avraham I, Dor Y, et al. VEGF-induced adult neovascularization: recruitment, retention, and role of accessory cells. *Cell*. 2006;124(1):175-189.
58. Dominici M, Rasini V, Bussolari R, et al. Restoration and reversible expansion of the osteoblastic hematopoietic stem cell niche after marrow radioablation. *Blood*. 2009;114(11):2333.
59. Abbott J, Huang Y, Liu D, Hickey R, Krause D, Giordano F. Stromal cell-derived factor-1a plays a critical role in stem cell recruitment to the heart after myocardial infarction but is not sufficient to induce homing in the absence of injury. Vol. 110: Am Heart Assoc; 2004:3300-3305.
60. Chitteti BR, Cheng YH, Poteat B, et al. Impact of interactions of cellular components of the bone marrow microenvironment on hematopoietic stem and progenitor cell function. *Blood*;115(16):3239.
61. Nakamura Y, Arai F, Iwasaki H, et al. Isolation and characterization of endosteal niche cell populations that regulate hematopoietic stem cells. *Blood*. 2010;116(9):1422-1432.
62. *Morrison MJKaSJ*. Uncertainty in the niches that maintain haematopoietic stem cells. *Nature Reviews Immunology*;8:290-301.
63. Van Overstraeten-Schlögel N, Beguin Y, Gothot A. Role of stromal-derived factor-1 in the hematopoietic-supporting activity of human mesenchymal stem cells. *European journal of haematology*. 2006;76(6):488-493.
64. Nakamura Y, Arai F, Iwasaki H, et al. Isolation and characterization of endosteal niche cell populations that regulate hematopoietic stem cells. *Blood*;116(9):1422.
65. Walters KB, Green JM, Surfus JC, Yoo SK, Huttenlocher A. Live imaging of neutrophil motility in a zebrafish model of WHIM syndrome. *Blood*. 2010;116(15):2803-2811.
66. Kobayashi I, Ono H, Moritomo T, Kano K, Nakanishi T, Suda T. Comparative gene expression analysis of zebrafish and mammals identifies common regulators in hematopoietic stem cells. *Blood*. 2010;115(2):e1-9.
67. Kobayashi I, Saito K, Moritomo T, Araki K, Takizawa F, Nakanishi T. Characterization and localization of side population (SP) cells in zebrafish kidney hematopoietic tissue. *Blood*. 2008;111(3):1131.
68. Huising MO, van der Meulen T, Flik G, Verburg-van Kemenade BML. Three novel carp CXC chemokines are expressed early in ontogeny and at nonimmune sites. *European Journal of Biochemistry*. 2004;271(20):4094-4106.
69. Baoprasertkul P, He C, Peatman E, Zhang S, Li P, Liu Z. Constitutive expression of three novel catfish CXC chemokines: homeostatic chemokines in teleost fish. *Molecular immunology*. 2005;42(11):1355-1366.
70. Westerfield M. *The Zebrafish Book. A Guide for the laboratory use of zebrafish (Danio rerio)*: Eugene: University of Oregon Press; 2000.

71. Liu Y, Pathak N, Kramer-Zucker A, Drummond I. Notch signaling controls the differentiation of transporting epithelia and multiciliated cells in the zebrafish pronephros. *Development*. 2007;134(6):1111.
72. Lawson ND, Weinstein BM. In vivo imaging of embryonic vascular development using transgenic zebrafish. *Developmental Biology*. 2002;248(2):307-318.
73. White RM, Sessa A, Burke C, et al. Transparent adult zebrafish as a tool for in vivo transplantation analysis. *Cell Stem Cell*. 2008;2(2):183-189.
74. Knaut H, Werz C, Geisler R. A zebrafish homologue of the chemokine receptor Cxcr4 is a germ-cell guidance receptor. *Nature*. 2003;421(6920):279-282.
75. Kawakami K, Shima A, Kawakami N. Identification of a functional transposase of the Tol2 element, an Ac-like element from the Japanese medaka fish, and its transposition in the zebrafish germ lineage. *Proceedings of the National Academy of Sciences of the United States of America*. 2000;97(21):11403-11408.
76. Paffett-Lugassy NN, and Zon, L.I. Analysis of hematopoietic development in the zebrafish. *Methods Mol Med*. 2004(105).
77. Zong Z-W, Cheng T-M, Su Y-P, et al. Recruitment of Transplanted Dermal Multipotent Stem Cells to Sites of Injury in Rats with Combined Radiation and Wound Injury by Interaction of SDF-1 and CXCR4. *Radiation Research*. 2009;170(4):444-450.
78. Dar A, Kollet O, Lapidot T. Mutual, reciprocal SDF-1/CXCR4 interactions between hematopoietic and bone marrow stromal cells regulate human stem cell migration and development in NOD/SCID chimeric mice. *Experimental Hematology*. 2006;34(8):967-975.
79. Juremalm M, Hjertson M, Olsson N, Harvima I, Nilsson K, Nilsson G. The chemokine receptor CXCR4 is expressed within the mast cell lineage and its ligand stromal cell-derived factor-1acts as a mast cell chemotaxin. *European Journal of Immunology*. 2000;30(12):3614-3622.
80. Bastianutto C, Mian A, Symes J, et al. Local radiotherapy induces homing of hematopoietic stem cells to the irradiated bone marrow. *Cancer research*. 2007;67(21):10112.
81. Ponomaryov T, Peled A, Petit I, et al. Induction of the chemokine stromal-derived factor-1 following DNA damage improves human stem cell function. *Journal of Clinical Investigation*. 2000;106(11):1331-1339.
82. Gupta R, Seith A, Guglani B. Renal hilar extramedullary hematopoiesis presenting as incidental unilateral renal hilar mass in adolescent male: a case report. *International urology and nephrology*. 2009;41(1):19-21.
83. Lotan D, Sheinberg N, Kopolovic J, Dekel B. Expression of SDF-1/CXCR4 in injured human kidneys. *Pediatric Nephrology*. 2008;23(1):71-77.
84. Gao C, Huan J. SDF-1 plays a key role in chronic allograft nephropathy in rats. *Transplantation Proceedings*. 2008;40(5):1674-1678.
85. Mazzinghi B, Ronconi E, Lazzeri E, et al. Essential but differential role for CXCR4 and CXCR7 in the therapeutic homing of human renal progenitor cells. *Journal of Experimental Medicine*. 2008;205(2):479-490.
86. Thomas' Hematopoietic Cell Transplantation: John Wiley & Sons; 2011.

87. Wong JY, Liu A, Schultheiss T, et al. Targeted total marrow irradiation using three-dimensional image-guided tomographic intensity-modulated radiation therapy: an alternative to standard total body irradiation. *Biol Blood Marrow Transplant*. 2006;12(3):306-315.
88. Somlo G, Spielberger R, Frankel P, et al. Total marrow irradiation: a new ablative regimen as part of tandem autologous stem cell transplantation for patients with multiple myeloma. *Clin Cancer Res*. 2011;17(1):174-182.
89. Travis EL, Peters LJ, McNeill J, Thames HD, Karolis C. Effect of dose-rate on total body irradiation: lethality and pathologic findings. *Radiother Oncol*. 1985;4(4):341-351.
90. Lehnert S, Rybka WB. Dose rate dependence of response of mouse lung to irradiation. *Br J Radiol*. 1985;58(692):745-749.
91. Peters LJ, Withers HR, Cundiff JH, Dicke KA. Radiobiological considerations in the use of total-body irradiation for bone-marrow transplantation. *Radiology*. 1979;131(1):243-247.
92. Hui SK, Verneris MR, Higgins P, et al. Helical tomotherapy targeting total bone marrow - first clinical experience at the University of Minnesota. *Acta Oncol*. 2007;46(2):250-255.
93. van Os R, Konings AW, Down JD. Compromising effect of low dose-rate total body irradiation on allogeneic bone marrow engraftment. *Int J Radiat Biol*. 1993;64(6):761-770.
94. Down JD, Tarbell NJ, Thames HD, Mauch PM. Syngeneic and allogeneic bone marrow engraftment after total body irradiation: dependence on dose, dose rate, and fractionation. *Blood*. 1991;77(3):661-669.
95. Collis SJ, Schwaninger JM, Ntambi AJ, et al. Evasion of early cellular response mechanisms following low level radiation-induced DNA damage. *J Biol Chem*. 2004;279(48):49624-49632.
96. Traver D, Winzeler A, Stern HM, et al. Effects of lethal irradiation in zebrafish and rescue by hematopoietic cell transplantation. *Blood*. 2004;104(5):1298-1305.
97. Glass T, Lund T, Patrinostro X, et al. Stromal cell-derived factor-1 (SDF-1) and hematopoietic cell homing in an adult zebrafish model of hematopoietic cell transplant. *Blood*. 2011.
98. Pei DS, Strauss PR. Zebrafish as a model system to study DNA damage and repair. *Mutat Res*. 2012.
99. Zeng Z, Richardson J, Verduzco D, Mitchell DL, Patton EE. Zebrafish have a competent p53-dependent nucleotide excision repair pathway to resolve ultraviolet B-induced DNA damage in the skin. *Zebrafish*. 2009;6(4):405-415.
100. Gillette-Ferguson I, Ferguson D, Poss K, Moorman S. Changes in gravitational force induce alterations in gene expression that can be monitored in the live, developing zebrafish heart. *Advances in Space Research*. 2003;32(8):1641-1646.
101. Pauls S, Geldmacher-Voss B, Campos-Ortega JA. A zebrafish histone variant H2A.F/Z and a transgenic H2A.F/Z:GFP fusion protein for in vivo studies of embryonic development. *Dev Genes Evol*. 2001;211(12):603-610.

102. Westerfield M. The Zebrafish Book: A Guide for the Laboratory Use of Zebrafish (Danio rerio). 2000: University of Oregon Press Eugene, OR.
103. Amundson SA, Grace MB, McLeland CB, et al. Human in vivo radiation-induced biomarkers: gene expression changes in radiotherapy patients. *Cancer Res*. 2004;64(18):6368-6371.
104. Amundson SA, Fornace AJ. Monitoring human radiation exposure by gene expression profiling: possibilities and pitfalls. *Health Phys*. 2003;85(1):36-42.
105. Lataillade JJ, Clay D, Dupuy C, et al. Chemokine SDF-1 enhances circulating CD34(+) cell proliferation in synergy with cytokines: possible role in progenitor survival. *Blood*. 2000;95(3):756-768.
106. Prise KM, O'Sullivan JM. Radiation-induced bystander signalling in cancer therapy. *Nat Rev Cancer*. 2009;9(5):351-360.
107. Khaled S, Gupta KB, Kucik DF. Ionizing radiation increases adhesiveness of human aortic endothelial cells via a chemokine-dependent mechanism. *Radiat Res*. 2012;177(5):594-601.
108. Cheng JC, Schultheiss TE, Wong JY. Impact of drug therapy, radiation dose, and dose rate on renal toxicity following bone marrow transplantation. *Int J Radiat Oncol Biol Phys*. 2008;71(5):1436-1443.
109. Pecaut MJ, Nelson GA, Gridley DS. Dose and dose rate effects of whole-body gamma-irradiation: I. Lymphocytes and lymphoid organs. *In Vivo*. 2001;15(3):195-208.
110. Pecaut MJ, Gridley DS, Smith AL, Nelson GA. Dose and dose rate effects of whole-body proton-irradiation on lymphocyte blastogenesis and hematological variables: part II. *Immunol Lett*. 2002;80(1):67-73.
111. Gridley DS, Pecaut MJ, Miller GM, Moyers MF, Nelson GA. Dose and dose rate effects of whole-body gamma-irradiation: II. Hematological variables and cytokines. *In Vivo*. 2001;15(3):209-216.
112. North TE, Goessling W, Walkley CR, et al. Prostaglandin E2 regulates vertebrate haematopoietic stem cell homeostasis. *Nature*. 2007;447(7147):1007-1011.
113. Scadden DT. Circadian rhythms: stem cells traffic in time. *Nature*. 2008;452(7186):416-417.
114. Yamazaki K, Allen TD. Ultrastructural morphometric study of efferent nerve terminals on murine bone marrow stromal cells, and the recognition of a novel anatomical unit: the "neuro-reticular complex". *Am J Anat*. 1990;187(3):261-276.
115. Kollet O, Shivtiel S, Chen Y, et al. HGF, SDF-1, and MMP-9 are involved in stress-induced human CD34+ stem cell recruitment to the liver. *Journal of Clinical Investigation*. 2003;112(2):160-169.
116. Winkler EA, Bell RD, Zlokovic BV. Central nervous system pericytes in health and disease. *Nat Neurosci*. 2011;14(11):1398-1405.
117. Davalos D, Grutzendler J, Yang G, et al. ATP mediates rapid microglial response to local brain injury in vivo. *Nat Neurosci*. 2005;8(6):752-758.